## Chapter 7

# Aberrations

Throughout the preceding chapters, we have come across the term *aberration*. We have mentioned that electron lenses are not perfect and talked in a rather unspecified manner about so-called lens effects, referring to defocus, spherical aberration and chromatic aberration. Spherical aberration and chromatic aberration are not the only aberrations which require our attention. Though spherical aberration is known to be the resolution-limiting aberration, it is only limiting in the sense that on conventional microscopes it cannot be corrected. On the other hand, it is a routine step towards an atomic-resolution micrograph to employ a stigmator in order to correct for twofold astigmatism, which, indeed, is also an aberration. However, due to the fact that it can be manually corrected to a precision where its residual impact can be ignored compared to the effect of spherical aberration, twofold astigmatism is rarely considered in the discussion of the image formation.

In aberration-corrected microscopes, it is commonly understood that the spherical aberration can be corrected. Hence, spherical aberration is not the resolution-limiting factor in such instruments anymore. This, however, does not mean that the microscope is free of aberrations, or that the point resolution becomes a meaningless quantity, or even a quantity which is determined solely by the wavelength or the diffraction limit. There are additional aberrations whose effects can become resolution-limiting. In fact, there is always at least one aberration which limits the optical resolution of a microscope. The ideal imaging instrument does not exist. Hence, with the advent of aberration-corrected electron microscopy, a need has emerged for understanding the individual residual aberrations of an aberration-corrected instrument. Microscopists who used to deal with spherical aberration and defocus have started to adopt the optical concepts which were previously mostly relevant for experts working in electron optics.

At this point it needs to be emphasized that besides optical effects, additional factors can be resolution-limiting in real electron microscopes. It is indeed often the case that the observable resolution is not limited primarily by the actual optical behavior of the instrument but by disturbances. Factors like the overall mechanical stability of the microscope or the stability of the electromagnetic lens fields generated by the microscope's power supplies can be decisive. Instabilities are particulary



ABERRATION-CORRECTED IMAGING IN TRANSMISSION ELECTRON MICROSCOPY - An Introduction
© Imperial College Press
http://www.worldscibooks.com/materialsci/p703.html

important if one aims at enhancing the resolution of a given microscope up to its theoretical optical limit. Moreover, in some cases it is even the specimen which imposes an unbreakable barrier to the observable resolution. In the present chapter, however, we accentuate the discussion on purely optical effects and presume that apart from such optical effects, the instrument behaves like an ideal noise-free instrument.

## 7.1 Overview

Figures 3.4 and 3.5, redrawn and summarized in Fig. 7.1, illustrate the blurring of the focal point of a non-ideal lens due to spherical aberration (Fig. 7.1a) and due to chromatic aberration (Fig. 7.1b). The identification of these aberrations essentially led us to the conclusion that electron lenses cause unwanted artifacts which demand our attention in the optical setup of the microscope, as well as in the discussion of the imaging characteristics of a particular microscope. For instance, in the presence of spherical aberration one preferably employs a defocus such that the disk of least confusion is imaged onto the Gaussian image plane. This is explained in detail in Chapter 3.

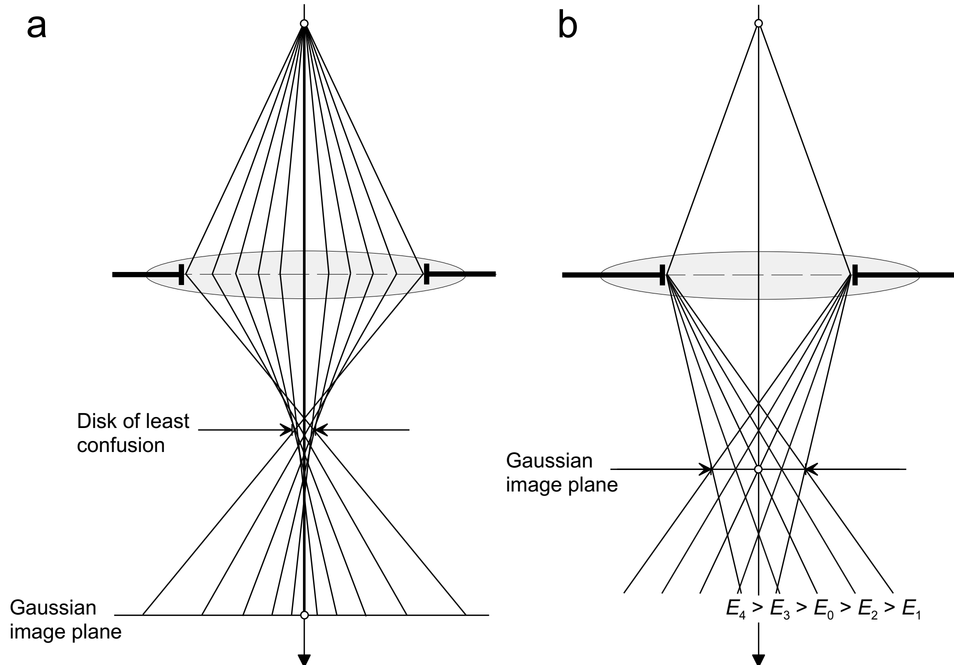


Fig. 7.1 Spherical aberration (**a**) and chromatic aberration (**b**).

ABERRATION-CORRECTED IMAGING IN TRANSMISSION ELECTRON MICROSCOPY - An Introduction
© Imperial College Press
http://www.worldscibooks.com/materialsci/p703.html

Spherical and chromatic aberrations impact the broad-beam phase-contrast imaging mode as well as the formation of the electron probe in scanning probe mode. While the spherical aberration determines the resolution (see Eqs. (2.32) and (3.11)), the chromatic aberration essentially limits the information transfer of high-frequent object information (see, e.g. Eq. (2.33) and Nellist and Pennycook, 1998). In any case, if aberrations are present and the energy spread of the beam is finite, the formation of a stigmatic image point reflecting an object point is not feasible.

On the other hand, we have seen in Chapter 6 that as long as the electrons stay close enough to the optical axis, i.e. close enough such that the Gaussian dioptrics is applicable, electromagnetic lenses can provide stigmatic images. As a matter of fact, a stigmatic image, i.e. an image where each object point is transferred to the image plane as a point such that the image is a (de)magnified and undistorted representation of the object, corresponds to the imaging characteristics that we would like to have. The possibility of stigmatic images is not in contradiction to the above argumentation. However, in order to produce images of *finite* resolution, it is necessary to consider electron trajectories that are at a small but finite distance to the optical axis or which run under a finite angle to the optical axis. The consideration of such rays complicates the situation. As soon as we start dealing with such rays we have to expand the conception about idealized imaging, which is essentially based on the paraxial approximation. As a consequence, we have to include higher-order terms in the description of the various trajectory equations. This was illustrated in Chapter 6, where we exemplified the effect of including terms of higher order in the trajectory equation for the simple case of the focusing strength of a homogeneous magnetic field (see Figs. 6.10 and 6.12). The rather simple expansion of the cosine function from the paraxial approximation $\cos\gamma = 1$ to $\cos\gamma = 1 - \gamma^2/2$ enabled us to derive an expression for the constant of spherical aberration of the homogeneous rotationally symmetric magnetic field. Hence, aberrations become effective when we treat a non-ideal imaging system beyond the paraxial approximation.

The above considerations essentially illustrate that aberrations describe the deviations from the optical behavior of an ideal instrument. The reference state, which provides an ideal image, is the imaging characteristics of the Gaussian optics, which is valid only within the paraxial approximation. As a matter of course, we choose the Gaussian optics, i.e. the optical behavior describable within the paraxial approximation, as our reference state. However, as will be shown, it is particularly evident to consider the paraxial approximation as this reference state when we generalize the idea of the aberration function and the concept of the geometrical wave surface, which we have already introduced in Chapters 2, 3 and 5. Nonetheless, having a well-defined reference state which is based on the Gaussian optics enables us to conceptually describe the term *aberration*.

ABERRATION-CORRECTED IMAGING IN TRANSMISSION ELECTRON MICROSCOPY - An Introduction
© Imperial College Press
http://www.worldscibooks.com/materialsci/p703.html

## 7.2 Image Aberrations

An electron ray is describable by two geometrical ray parameters; the complex coordinate in the aperture plane $\omega$ and the position of the trajectory in the object plane, which, in analogy to $\omega = \theta_x + \mathrm{i}\theta_y$, we describe by a complex coordinate $w_\mathrm{o} = x_\mathrm{o} + \mathrm{i}y_\mathrm{o}$. Knowing $\omega$ and $w_\mathrm{o}$, the Gaussian optics can be applied to derive the position of a ray in the Gaussian image plane. This position, also described by a complex value $w_\mathrm{i} = x_\mathrm{i} + \mathrm{i}y_\mathrm{i}$, corresponds to the Gaussian image point which reflects the object point $w_\mathrm{o}$ in the object plane, i.e. the source point of the trajectory[1]. An aberrated ray does not intersect the Gaussian image plane in $w_\mathrm{i}$ but in a point $w_\mathrm{i}'$. This is the basis of the definition of the image aberrations; the *image aberration* $\Delta w_\mathrm{i}$ is the distance between the location where the Gaussian ray intersects the Gaussian image plane and the location where the actual (aberrated) ray intersects the Gaussian image plane, i.e.

$$\Delta w_\mathrm{i} = w_\mathrm{i}' - w_\mathrm{i}. \tag{7.1}$$

This is illustrated in Fig. 7.2.

Each aberration has a characteristic aberration figure which can depend on the location of the object point $w_\mathrm{o}$ as well as on the location $\omega$ in the aperture plane where a ray intersects the aperture plane.

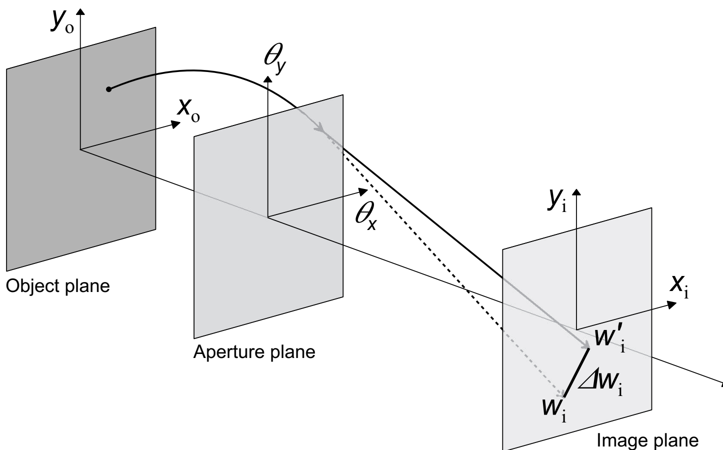


Fig. 7.2 Definition of the image aberration $\Delta w_\mathrm{i}$. The paraxial or Gaussian ray (dashed line) intersects the Gaussian image plane in $w_\mathrm{i}$, while the aberrated ray (full line) hits the plane in $w_\mathrm{i}'$. The difference corresponds to the image aberration of the ray $\Delta w_\mathrm{i}$.

[1] In the foregoing text, we do not strictly specify whether the cartesian coordinate $(x, y)$ is in the object or image plane. From the context it should be clear which plane is meant. However, whenever needed, we employ subscripts in the complex coordinate $w_\mathrm{o}$ and $w_\mathrm{i}$ to elucidate whether object or image plane is meant.

ABERRATION-CORRECTED IMAGING IN TRANSMISSION ELECTRON MICROSCOPY - An Introduction
© Imperial College Press
http://www.worldscibooks.com/materialsci/p703.html

## 7.3 Types of Aberrations

Aberrations have different facets and they affect the imaging process in various ways, but they all have in common that at least for one set of geometrical ray parameters $(\omega, w_\mathrm{o})$, the image aberration $\Delta w_\mathrm{i} \neq 0$. There are aberrations which are sensitive to the wavelength of the electrons, aberrations which depend on the scattering or illumination angle and aberrations which depend on the location of the object point within the object plane. There are aberrations which alter the coherence between the electrons in the beam and aberrations which do not influence coherency. It seems obvious therefore to distinguish aberrations according to their effect on electrons. Hence, for now we shall be concerned with the classification of aberrations.

### 7.3.1 *Axial aberrations vs. off-axial aberrations*

The aberrations we have considered so far are defocus, spherical aberration and chromatic aberration. They have a common characteristic: regardless of whether they impact a STEM probe or the imaging process in TEM, their effect increases with the inclination angle of the electron trajectories in respect to the optical axis. The impact of defocus and spherical aberration is described by the aberration function which is given for HRTEM and STEM in Eqs. (2.16) and (3.14), respectively, and which can be rewritten as

$$\chi(\theta) = \frac{1}{2}\theta^2 C_1 + \frac{1}{4}\theta^4 C_3.$$

Here, $\theta$ shall be the scattering angle in HRTEM as well as the illumination angle of a particular electron trajectory in STEM. Employing the notation of the complex angle $\omega$ for the angle $\theta$

$$\chi(\omega) = \Re\left(\frac{1}{2}\omega\overline{\omega}C_1 + \frac{1}{4}\left(\omega\overline{\omega}\right)^2 C_3\right),$$

we obtain a two-dimensional description of the effect of defocus and spherical aberration of third order, where $\omega$ and $\overline{\omega}$ are the complex angle and its complex conjugate according to Fig. 2.7. The complex angle $\omega$ is the two-dimensional position coordinate of an electron trajectory in the aperture plane. For STEM, the aperture plane is in front of the specimen conjugate to the front focal plane of the objective lens, and for HRTEM, the aperture plane is the back focal plane of the objective lens. The angle $|\omega| = |\theta_x + \mathrm{i}\theta_y| = \theta$ essentially defines the inclination angle of an electron trajectory in respect to the optical axis at the object plane, irrespective of the point in the object plane.

The behavior of the chromatic aberration is similar: the effect of the chromatic aberration increases with the angle $|\omega|$ as well. This can be seen from Eq. (3.6); the impact of the chromatic aberration increases linearly with the illumination semi-angle $\alpha$ and thus with $|\omega|$. For the case of HRTEM, it is the envelope function due to partial temporal coherence which describes the effect of the chromatic aberration.

ABERRATION-CORRECTED IMAGING IN TRANSMISSION ELECTRON MICROSCOPY - An Introduction
© Imperial College Press
http://www.worldscibooks.com/materialsci/p703.html

According to Eq. (2.24), the incoherent dampening of the coherent transfer increases with the scattering angle $\theta$ or with $|\omega|$, respectively. Furthermore, we recall that the spread of defocus $\Delta C_1$ is proportional to $C_C$ (see Eq. (2.23)). Hence, the effect of the chromatic aberration $C_C$ increases with the scattering angle.

Defocus $C_1$, spherical aberration $C_3$ and chromatic aberration $C_C$ thus have in common that their effects on the STEM probe or on a HRTEM image depend on the illumination or scattering angle, i.e. on the position coordinate $\omega$ in the respective aperture plane. However, their effects do not depend on the position in the object plane $w_o = x_o + iy_o$. Indeed, all object points $w_o$ and all image points $w_i$ are identically affected by these aberrations. For $C_1$, $C_3$ and $C_C$, the relevant position variable or the relevant geometrical ray parameter is the position $\omega$ in the aperture plane. An aberration whose effect is solely a function of the position coordinate in the aperture plane (STEM or HRTEM) is called an *aperture* aberration or an *axial* aberration. Defocus $C_1$, spherical aberration $C_3$ and chromatic aberration $C_C$ are axial aberrations[2]. On the other hand, an aberration whose effect depends on the position $w_o$ in the object plane (and possibly on the position in the aperture plane as well) is called an *off-axial* aberration.

*The isoplanatic approximation*

In the previous discussion about lens effects, we have dealt with axial aberrations only and thus assumed that for all object points which are imaged onto the image plane, the same transfer function is valid. Hence, implicitly we expect the same resolution for all image points. This assumption, which is called the *isoplanatic* approximation, is of course only justifiable if all relevant aberrations are axial aberrations. In the presence of off-axial aberrations, the resolution is not equal for all image points and the isoplanatic approximation fails. This applies to TEM imaging as well as to STEM imaging.

Considering the fact that the electromagnetic fields in electron microscopes are rather inhomogeneous with a distinct radial dependence, and considering the fact that the specimen in a transmission electron microscope is immersed in the field of the objective lens, it almost seems to be a surprise that the isoplanatic approximation holds at all. Indeed, it holds so well that it is very often implicitly presumed and not even mentioned in the literature about the image formation in HRTEM. The reason for this lies in the high magnifications employed to do HRTEM imaging and atomic-resolution STEM imaging. The bore of a high-resolution objective lens is typically 2 to 3 mm in diameter (see, e.g. Fig. 6.13), while the field of view of a high-resolution micrograph is typically less than 100 nm. Hence, the field of view is four orders of magnitude smaller than the spatial extension of the electromagnetic field within the bore. It is for this reason that off-axial aberrations can often be ignored such that the entire object area imaged in a high-resolution micrograph can

[2] This statement already implies a simplification concerning the chromatic aberration, which is resolved in the following section.

ABERRATION-CORRECTED IMAGING IN TRANSMISSION ELECTRON MICROSCOPY - An Introduction
© Imperial College Press
http://www.worldscibooks.com/materialsci/p703.html

be considered to be affected by a transfer function which in principle is only valid for the central point of the object plane.

Though the isoplanatic approximation holds reasonably well in high-resolution imaging, as with any approximation, it has, of course, its limitation. This limitation reasons the definition of a slightly longish term that is known as the *number of equally well resolved image points*. The maximum number of equally well resolved image points, measured along the diameter of the recorded image, defines the largest field of view for which the isoplanatic approximation holds. For a field of view which exceeds the maximum number of equally well resolved image points, the effect of off-axial aberrations becomes the resolution limiting factor, i.e. for points beyond the maximum number of equally well resolved image points.

### 7.3.2 *Chromatic aberrations vs. geometrical aberrations*

We have already come across the term 'chromatic aberration' and discussed the effect of $C_C$ for HRTEM as well as for STEM imaging. The chromatic aberration is usually referred to as an incoherent aberration, which essentially implies that it leads to a loss of information. This is, for instance, expressed by the fact that the chromatic aberration limits the information transfer in HRTEM imaging. In STEM, the chromatic aberration essentially enhances the intensity of the side lobes of the electron probe. This leads mainly to the same effect as in HRTEM imaging, i.e. it reduces the contrast of high-resolution information (see, e.g. Nellist and Pennycook, 1998). There are other incoherent aberrations which are not actual optical effects; mechanical vibrations, the finite size of the electron source, instabilities of the power supplies used to feed the electron optical elements, specimen drift or the information loss due to the point spread function of the detector. All these issues can be considered to be incoherent aberrations as well. Similarly to the chromatic aberration, these additional incoherent aberrations lead to a loss of information.

The effect of the chromatic aberration increases with decreasing electron energy and increasing energy spread of the beam. The energy spread of conventional field-emission electron microscopes is, however, sufficiently narrow such that when operating the microscope above about 100 kV, the chromatic aberration imposes a limit on the information transfer (see Eq. (2.33)) but not on the resolution. Hence, though the chromatic aberration can in principle limit the resolution of a microscope, for dedicated high-resolution microscopes this is normally not the case. For typical transmission electron microscopes, Eqs. (2.32) and (3.11) define the point resolution for HRTEM imaging and for STEM imaging, respectively. Hence, it is the spherical aberration of the objective lens which imposes a limit on the achievable resolution.

The spherical aberration is a geometrical aberration. Geometrical aberrations, which are also referred to as coherent aberrations, do not necessarily lead to an actual loss of information. They primarily affect the interpretability of the

ABERRATION-CORRECTED IMAGING IN TRANSMISSION ELECTRON MICROSCOPY - An Introduction
© Imperial College Press
http://www.worldscibooks.com/materialsci/p703.html

micrographs. As we have already seen in Chapters 2, 3 and 4, coherent (axial) aberrations cause a phase shift of the electron wave in the respective aperture plane, leading to a displacement of the electron trajectories from the non-aberrated trajectories. This becomes particularly clear when we consider HRTEM imaging, where the delocalization due to the oscillating phase contrast transfer function complicates the interpretability of phase contrast micrographs. The point resolution given in Eq. (2.32), which defines the smallest distance that can directly be resolved and interpreted, is typically larger than the information limit given in Eq. (2.33). Hence, since the information limit exceeds the point resolution, a typical HRTEM micrograph contains information beyond the point resolution. The information between point resolution and information limit is not lost, but because of the effect of the geometrical aberrations, namely the spherical aberration, it is not directly interpretable. Employing rather complex restoration procedures on series of micrographs each recorded under slightly different imaging conditions, the information between point resolution and information limit can be restored. Such restoration techniques thus allow for numerically extending the resolution of a microscope up to the information limit of the instrument, provided all relevant geometrical aberrations are known with sufficient precision (see Chapter 4). The possibility of restoring the aberrated image information in the presence of coherent aberrations is in contrast to incoherent aberrations, like the chromatic aberration, which lead to an actual loss of information that cannot be restored.

#### 7.3.2.1 *Chromatic aberrations*

Figure 7.1b illustrates that the chromatic aberration causes the focal point of a lens to change with the electron energy and thus with the wavelength of the electrons. We have also seen that the effect of the chromatic aberration $C_\mathrm{C}$ is an axial effect and that it can be described in the aperture plane, respectively in the front- or back-focal plane of the objective lens depending on whether we do STEM or HRTEM. However, what we called simply the chromatic aberration $C_\mathrm{C}$ and schematically illustrated in Fig. 7.1b is in fact only one particular aspect of the overall chromatic effects that can occur in an electron optical instrument. Though $C_\mathrm{C}$ as illustrated in Fig. 7.1b is often the dominant chromatic effect, there is not a *single* chromatic aberration. There are chromatic aberrations.

In principle, any lens effect which depends on the *chromatic parameter* $\kappa$

$$\kappa = \frac{\delta E}{E_0} \tag{7.2}$$

is a chromatic aberration. The chromatic parameter describes the relative energy deviation of an electron in respect to the nominal electron energy $E_0$, where $\delta E$ is the deviation from $E_0$. If a certain functionality of an instrument does not depend on $\kappa$, it is an achromatic functionality or, more generally, an *achromatic* effect.

For the case in which the effect of a particular chromatic aberration depends only on the scattering (or illumination) angle $\omega$, the aberration is called an axial

ABERRATION-CORRECTED IMAGING IN TRANSMISSION ELECTRON MICROSCOPY - An Introduction
© Imperial College Press
http://www.worldscibooks.com/materialsci/p703.html

chromatic aberration or a chromatic aperture aberration. On the other hand, if the effect of a chromatic aberration depends on the position $w_o$ in the object plane, it is called a chromatic distortion or an off-axial chromatic aberration, as discussed in the previous section.

What we called simply the coefficient of chromatic aberration $C_C$ is indeed the primary axial chromatic aberration $C_{C\,1}$, whose impact is isotropic. Equation (3.6), rewritten as

$$\delta_C = C_{C\,1}\,\theta\,\frac{\delta E}{E_0} = C_{C\,1}\,|\omega|\,\frac{\delta E}{E_0},$$

describes the blurring of the focal point in the Gaussian image plane due to the primary axial chromatic aberration $C_{C\,1}$. While the above relation describes the radius of the circle of confusion in the Gaussian image plane (see Eq. (3.6)), the image aberration $\Delta w_i$ can be expressed as (see, e.g. Typke and Dierksen, 1995)

$$\Delta w_i = -M C_{C\,1}\,\omega\,\kappa, \tag{7.3}$$

where we substituted $\delta E/E_0$ with the chromatic parameter $\kappa$. The factor $M$ in Eq. (7.3) is the lateral magnification[3].

We see that the impact of the chromatic aberration $C_{C\,1}$ depends linearly on the geometrical ray parameter $\omega$ and on the chromatic parameter $\kappa$. Since according to Eq. (7.2) the chromatic parameter increases with decreasing nominal electron energy $E_0$, by choosing a sufficiently high microscope high tension, the effect of the chromatic blurring can be reduced such that it is not the resolution-defining quantity.

*Order, degree and rank*

The *order* $n$ of an aberration can be defined as the sum of the exponents of the geometrical ray parameters which describe the effect of the aberration in the image plane, i.e. its image aberration $\Delta w_i$ (Rose, 2009a). For STEM, the image plane, i.e. the plane where the demagnified image of the source is formed, is the specimen plane, which for HRTEM is the actual object plane. The geometrical ray parameters are the coordinate in the aperture plane $\omega$ and the coordinate in the object plane $w_o$. Since the effect of the primary axial chromatic aberration depends linearly on the geometrical ray parameter $\omega$ (see Eq. (7.3)), its order $n = 1$. Hence, $C_{C\,1}$ is a first-order aberration. The numerical subscript 1 thus indicates the order $n$ of the aberration. Furthermore, the *degree* of an aberration is equal to the exponent of

[3]The reason why the magnification $M$ needs to be incorporated in the description of the image aberration lies in the fact that the aberration coefficients are defined in terms of the object plane. This makes the aberration coefficient independent of the magnification $M$. Incorporating the magnification in Eq. (7.3) means that $\Delta w_i$ describes the (size of the) aberration figure in the image plane, as for instance defined by the fluorescence screen. On the other hand, it is also quite common to omit the magnification in the equation of the image aberrations, which means that the image aberrations are then described in a plane referred back to the object with $M = 1$ (see, e.g. Hawkes, 2009b). This is discussed in more detail in Sec. 7.4.0.1.

ABERRATION-CORRECTED IMAGING IN TRANSMISSION ELECTRON MICROSCOPY - An Introduction
© Imperial College Press
http://www.worldscibooks.com/materialsci/p703.html

the chromatic parameter $\kappa$, which is used to describe the effect of the aberration in the image plane. For the case of $C_{\mathrm{C}\,1}$, the degree is equal to 1. Finally, the *rank* of an aberration is the sum of the degree and the order of the aberration. Hence, $C_{\mathrm{C}\,1}$ is a second-rank aberration. Besides, with the introduction of the degree of an aberration, we can simply define chromatic aberrations as aberrations whose degree is larger than zero.

The effect of the primary axial chromatic aberration is illustrated in Fig. 7.1b; it causes an object point to be imaged in the image plane as a disk because the focal point varies with electron energy. This is the dominant chromatic aberration of a round lens[4]. Apart from the axial chromatic aberration $C_{\mathrm{C}\,1}$, in general round electron lenses possess contributions of off-axial chromatic aberrations which show a distortion character. These non-aperture chromatic aberrations, or chromatic distortions, are described by the coefficient of chromatic aberration of magnification $C_{\mathrm{D}}$ and the anisotropic chromatic distortion coefficient $C_{\theta}$, which, for purely electrostatic electron lenses, is zero (Hawkes and Kasper, 1989a). $C_{\mathrm{D}}$ and $C_{\theta}$ can be summarized in a complex quantity $A_{\mathrm{C}\,1\,1} = C_{\mathrm{D}} + \mathrm{i}C_{\theta}$, which is the chromatic magnification change (Typke and Dierksen, 1995). While the first numerical index of $A_{\mathrm{C}\,1\,1}$ refers to the order of the aberration as described above, the second numerical subscript indicates the power of $w_{\mathrm{o}}$ appearing in the relation of the corresponding image aberration $\Delta w_{\mathrm{i}}$. The second numerical subscript thus describes the dependency of the aberration on the object position $w_{\mathrm{o}}$. For axial chromatic aberrations this value is zero, and is thus omitted. The subscript C indicates a chromatic aberration.

For conventional electron microscopes consisting of round optical elements, the axial chromatic aberration $C_{\mathrm{C}\,1}$ is the dominant chromatic aberration. The effects of other chromatic aberrations, like $A_{\mathrm{C}\,1\,1}$, are usually negligible. This reasons the usage of the notation $C_{\mathrm{C}}$ for $C_{\mathrm{C}\,1}$ and its colloquial naming as the chromatic aberration. However, besides the isotropic axial aberration $C_{\mathrm{C}\,1}$, for non-round electron lenses additional axial chromatic aberrations are feasible. Examples of these are the dispersion $A_{\mathrm{C}\,0}$ and the chromatic twofold astigmatism $A_{\mathrm{C}\,1}$. The chromatic aberrations $C_{\mathrm{C}\,1}$, $A_{\mathrm{C}\,0}$ and $A_{\mathrm{C}\,1}$ are axial chromatic aberrations and thus do not depend on $w_{\mathrm{o}}$. This reasons the omission of the second numerical subscript. While $C_{\mathrm{C}\,1}$ leads to a change of defocus with changing electron energy (see Fig. 3.5), the dispersion $A_{\mathrm{C}\,0}$ leads to an image shift with changing energy and $A_{\mathrm{C}\,1}$ induces twofold astigmatism whose amount depends on the energy of the electron. Dispersion $A_{\mathrm{C}\,0}$ is an aberration of order zero and rank one, whereas the chromatic twofold astigmatism $A_{\mathrm{C}\,1}$ is a first-order aberration of rank two. All chromatic aberrations discussed are of first degree, i.e. they depend linearly on the chromatic parameter $\kappa$.

With this we close our short excursion into the field of chromatic aberrations. The essential point about this section is that there is not a single chromatic

[4]The term *round* lens can be misleading. What we mean by *round* lens is a lens which produces a rotationally symmetric electromagnetic field that is used to control the path of the electron beam.

ABERRATION-CORRECTED IMAGING IN TRANSMISSION ELECTRON MICROSCOPY - An Introduction
© Imperial College Press
http://www.worldscibooks.com/materialsci/p703.html

aberration, as commonly presumed in the literature. In fact, the reduction of the overall chromatic effect of a round electron lens to a single quantity $C_\mathrm{C}$ is only justifiable because there is a dominant chromatic aberration, which is the isotropic axial chromatic aberration $C_{\mathrm{C}\,1}$. Furthermore, the impact of $C_{\mathrm{C}\,1}$ does not vanish for object points close to the optical axis. Hence, even at very high magnifications, where in principle off-axial (chromatic) aberrations are negligible, $C_{\mathrm{C}\,1}$ needs to be taken into account.

The topic of chromatic aberrations has many more facets than have been elucidated here briefly. Particularly in the case of non-round optical elements and in the discussion of energy filters, the proper treatment of chromatic aberrations is essential. For an extended discussion of chromatic aberrations, the reader is referred to more advanced electron-optical texts, as can be found in Hawkes and Kasper (1989a), Rose and Krahl (1995), Hawkes (2007) and Rose (2009a). In particular, for a complete derivation of all aberrations up to second rank, including geometrical aberrations, see Rose (2009a).

#### 7.3.2.2 *Geometrical aberrations*

We essentially defined the chromatic aberrations as aberrations which depend on the relative energy of the electrons and thus depend on the chromatic parameter $\kappa$. This dependency is described by the degree of an aberration which for chromatic aberrations is greater than zero. Since the rank of an aberration is the sum of its order and its degree, the rank of a chromatic aberration is thus greater than its order. *Geometrical* aberrations, on the other hand, do not depend on the relative energy of the electrons. Their impact depends solely on the geometrical ray parameters $\omega$ and $w_\mathrm{o}$. The degree of geometrical aberrations thus vanishes and the order of a geometrical aberrations is equal to its rank.

Geometrical aberrations lead to well defined phase shifts of electron rays. The phase shifts depend on the geometrical ray parameters that define a given ray. Rays of different ray parameters can thus undergo different phase shifts. Letting these rays interfere either to form a HRTEM micrograph or a STEM probe reveals the various phase shifts in the form of an aberrated micrograph or an aberrated STEM probe. The coherence between different electron trajectories is not affected by the purely geometrical effect of these aberrations. This reasons why geometrical aberrations are also called coherent aberrations.

We have seen that the effects of defocus $C_1$ and third-order spherical aberration $C_3$ do not depend on the chromatic parameter $\kappa$. Hence, $C_1$ and $C_3$ are geometrical aberrations. Figures 7.1a and 6.12 illustrate the effect of spherical aberration; the focal point depends on the geometrical parameter $\omega$ in the aperture plane. While the focal point of the trajectory along the optical axis, i.e. the paraxial trajectory, defines the Gaussian focal point, for rays with $|\omega| \neq 0$, the effective focal distance is shorter than the one for the rays with $|\omega| \to 0$. With increasing $|\omega|$, the effective focal distance decreases. Furthermore, since according to Eqs. (2.16) and (3.14)

ABERRATION-CORRECTED IMAGING IN TRANSMISSION ELECTRON MICROSCOPY - An Introduction
© Imperial College Press
http://www.worldscibooks.com/materialsci/p703.html

the effects of $C_1$ and $C_3$ do not depend on the position $w_o$ in the object plane, $C_1$ and $C_3$ are a special type of geometrical aberration, namely axial aberrations. The image aberrations $\Delta w_i$ (see Fig. 7.2) due to defocus $C_1$ and third-order spherical aberration $C_3$ can be written as

$$C_1: \quad \Delta w_i = -MC_1\omega$$
$$C_3: \quad \Delta w_i = -MC_3\overline{\omega}\omega^2. \tag{7.4}$$

The above relations reveal that the effect of defocus $C_1$ in the image plane depends linearly on the geometrical ray parameter $\omega$. Hence, $C_1$ is a first-order axial aberration. On the other hand, since the effect of $C_3$ depends on $\overline{\omega}\omega^2$, its order is three. This is reflected in their respective numerical subscripts.

*Geometrical aberrations vs. parasitic aberrations*

A further distinction between actual geometrical aberrations and *parasitic* aberrations is feasible. According to Hawkes (2007), the first category, i.e. geometrical aberrations, describes the permitted aberrations of an ideal optical element of a given symmetry. An optical element of a given symmetry can only lead to a certain amount of aberrations, which are predetermined by its symmetry. Which type of aberrations are feasible for a given symmetry is discussed in detail by Hawkes and Kasper (1989b). For round electron lenses, the possible aberrations are the so-called Seidel aberrations, which are discussed in a forthcoming section of this chapter. Hence, according to Hawkes (2007), coherent aberrations which are permitted by the symmetry of the optical element represent the actual geometrical aberrations.

*Parasitic* aberrations, on the other hand, are aberrations which are induced by mechanical imperfections or, for instance, by inhomogeneities of the magnetic material the poles are made of. Hence, even though a given optical element theoretically can only cause a well defined set of symmetry-allowed aberrations, in practice it can cause a much larger variety of aberrations because no lens can ever be perfectly machined. The effect of these coherent parasitic aberrations depends on the geometrical ray parameters but not on the chromatic parameter $\kappa$.

Nonetheless, the differentiation between parasitic and symmetry-permitted aberrations can also be applied to (incoherent) chromatic aberrations. While an ideal round electron lens can only possess non-vanishing coefficients $C_{C\,1}$ and $A_{C\,1\,1}$ (up to second rank), i.e. the primary axial chromatic aberration and the chromatic magnification change, for non-ideal round electron lenses other chromatic aberration contributions could appear, like for instance the chromatic twofold astigmatism $A_{C\,1}$. Furthermore, any mechanical instability or the instability of the electromagnetic fields that form the optical units in an electron microscope can in principle be regarded as incoherent parasitic aberrations.

Another example which elucidates the difference between parasitic and symmetry permitted aberrations can be recognized in the standard alignment routine of

ABERRATION-CORRECTED IMAGING IN TRANSMISSION ELECTRON MICROSCOPY - An Introduction
© Imperial College Press
http://www.worldscibooks.com/materialsci/p703.html

an electron microscope. Doing high-resolution imaging in the broad-beam TEM mode or in STEM mode, it is unavoidable to correct for twofold axial astigmatism, which either directly impairs the image formation in HRTEM or the STEM probe and thus indirectly influences the respective micrographs. This astigmatism is a geometrical axial aberration which, however, is not permitted by the symmetry of a round objective lens. While the geometrical aberrations permitted by a round electron lens are discussed in the next section, axial twofold astigmatism is a direct consequence of the lens' deviation from producing a perfectly rotationally symmetric electromagnetic field. Hence, twofold axial astigmatism is a parasitic aberration which can be of importance in (conventional) atomic-resolution electron microscopy.

In the foregoing text we limit our treatise to geometrical aberrations. First, we will discuss the so-called Seidel aberrations of a round electron lens. Then, we will generalize the concepts of the geometrical wave front and the aberration function, in order to describe the optical behavior of electron optical elements of lower symmetry. This will lead us to the (residual) geometrical aberrations which have to be considered in aberration-corrected electron microscopy.

## 7.4 Geometrical Aberration of a Round Electron Lens

The number of geometrical aberrations an optical element possesses is in principle infinite. However, the amount of aberrations, or aberration coefficients, that need to be considered in the practical treatment of a particular optical system depends on the geometrical ray parameters that are of importance for the image formation. In general, the number increases with the precision by which the electron optical system needs to be described. It increases with the resolution of the optical system. For a limited regime of geometrical ray parameters, which is determined by the design of the optical instrument, one can assume that certain aberrations are of importance and need to be considered in the discussion of the image formation while others are not. Aberrations that are negligible are the ones which do not significantly affect rays within the relevant range of geometrical ray parameters $\omega$ and $w_o$.

In transmission electron microscopy, one is not interested in how a lens field acts on electrons that are scattered to large angles or on electrons which are even back-scattered. In fact, one is interested only in how the lens field acts on rays which are describable by small $\omega$ and small $w_o$. Hence, for the treatment of practical (electron-) optical instruments, one can reduce the problem. The way to do this is to consider aberrations up to a certain order. This essentially means that in electron optics, one is interested in aberrations whose effect on the image (or on the electron probe) depend on first, second and third power on the ray parameters, i.e. one is interested in aberrations that are of first, second and third order. However, with increasing resolution, the regime of the ray parameters needs to be expanded such that higher-order aberrations, i.e. fourth- and fifth-order aberrations, need to

ABERRATION-CORRECTED IMAGING IN TRANSMISSION ELECTRON MICROSCOPY - An Introduction
© Imperial College Press
http://www.worldscibooks.com/materialsci/p703.html

be considered as well. This is also important if the symmetry of the system deviates from its ideal design (see, e.g. Rose, 1968a, 1968b).

Ludwig Seidel is commonly said to be the first person who analyzed the permitted geometrical aberrations up to third order of a round light optical lens. The work he carried out around 1855 was published in 1857 under a rather lengthy title[5]. Yet, it has to be mentioned that Joseph Maximilian Petzvals performed an equivalent analysis prior to Seidel's work. However, Petzvals' manuscript was lost even before it could be published. Hence, the primary geometrical aberrations up to third order of a round lens are commonly said to be the *Seidel aberrations*.

Seidel performed the analysis for a light optical lens, which, however, has fewer aberration coefficients than the electron optical equivalent in the presence of magnetic fields. Nonetheless, the naming has been adopted to describe the aberrations up to third order of a round electron optical lens as well.

The amount of geometrical aberration coefficients up to third order of a round light optical lens is five (Born and Wolf, 2001), whereas in the presence of magnetic fields, a round electron lens can possess up to eight (Hawkes and Kasper, 1989a). Hence, in general, eight geometrical aberration coefficients have to be considered in order to describe the optical behavior of an ideal round electron lens up to third order. The following aberrations can be distinguished; spherical aberration, coma, field astigmatism, field curvature and distortion. In the foregoing subsections, the effects of these aberrations are discussed on a qualitative basis. The reference is the Gaussian optics where a point in the object plane is imaged as a point in the image plane. The ideal, i.e. stigmatic image point in the image plane, is called the Gaussian image point. For TEM, the object plane corresponds to the plane where the specimen is located, the corresponding aperture plane is the back focal plane of the objective lens, and the image plane is the plane where the detector is located. In STEM, the object plane is essentially a plane that corresponds to the plane of the electron source, and the image plane is the plane where the electron probe is brought to focus, i.e. the plane of the specimen. Hence, it is the image of the electron source projected onto the specimen plane which is affected by the lens aberrations in STEM mode and thus ultimately limits the STEM resolution. The relevant aperture plane in STEM is the front focal plane of the objective lens. Hence, when we talk about the impact of the aberrations on the image plane, we mean in TEM mode the plane of the detector, while for STEM it is the specimen plane. The relevant aperture planes are the front focal plane for STEM and the back focal plane for HRTEM, respectively.

[5]The title of Seidel's work is *Über die Theorie der Fehler, mit welchen die durch optische Instrumente gesehenen Bilder behaftet sind, und über die mathematischen Bedingungen ihrer Aufhebung* (in Abhandlungen der naturwiss.-techn. Commission bei der Königl. Bayerischen Akademie der Wissenschaften in München, Nr. 1. (1857) 227–267), which can be translated as *On the Theory of Errors by which Images Observed by Optical Instruments are Affected and on the Mathematical Conditions on Their Annihilation.*

ABERRATION-CORRECTED IMAGING IN TRANSMISSION ELECTRON MICROSCOPY - An Introduction
© Imperial College Press
http://www.worldscibooks.com/materialsci/p703.html

#### 7.4.0.1 *Spherical aberration*

We have already discussed the impact of the spherical aberration and illustrated its effect in Fig. 7.1a. The aberration figure in the image plane associated with spherical aberration is a disk which is centered at the Gaussian image point. In fact, each set of rays that passes the aperture plane under a given angle $|\omega|$ forms a circle in the Gaussian image plane. The radius $r_\mathrm{S}$ of the circle that is formed by rays that pass the aperture plane in $|\omega|$ is

$$r_\mathrm{S} = MC_3|\omega|^3, \tag{7.5}$$

while the actual image aberration is described by

$$\Delta \mathrm{w_i} = -MC_3\overline{\omega}\omega^2. \tag{7.6}$$

If an aperture of opening $|\omega_\mathrm{a}| = \theta_\mathrm{a}$ is employed, Eq. (7.5) provides the radius of the resulting aberration figure in the image plane. This disk reflects the astigmatic image point corresponding to a single point of the object. Hence, each object point is imaged as a disk of finite radius. The radius of the disk depends neither on the position of a particular point in the object plane nor on the position in the image plane. This is illustrated in Fig. 7.3. The quantity $C_3$ in Eq. (7.5) is the constant of spherical aberration, and $M$ is the lateral magnification. Because the impact of $C_3$ in the image plane scales with the third power of the ray parameter $|\omega|$, $C_3$ is the constant of spherical aberration of third order, i.e. it is the quantity $C_\mathrm{S}$ which is often used in the literature to refer to spherical aberration. Here, however, we would like to emphasize the order of the aberration which is denoted by the numerical subscript. Since the impact of $C_3$ is independent of the coordinate $w_\mathrm{o}$ in the object plane, the second numerical subscript, as introduced in the discussion of the chromatic aberrations, is equal zero and is thus omitted.

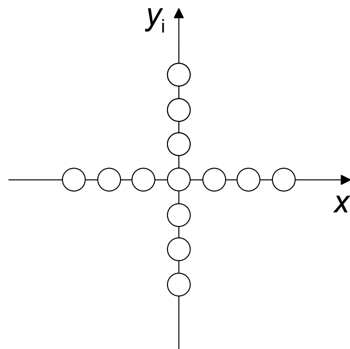


Fig. 7.3 The effect of spherical aberration $C_3$ on object points imaged onto the image plane $w_\mathrm{i} = x_\mathrm{i} + \mathrm{i}y_\mathrm{i}$. Each object point results in a disk. The radius of the disk depends neither on the position of the object point nor on the position of the image point in the image plane. The radius depends solely on the opening of the aperture, as described by Eq. (7.5).

ABERRATION-CORRECTED IMAGING IN TRANSMISSION ELECTRON MICROSCOPY - An Introduction
© Imperial College Press
http://www.worldscibooks.com/materialsci/p703.html

The lateral magnification appearing in Eqs. (7.5) and (7.6) requires a short explanation. The aberration coefficients, such as $C_3$, are defined in terms of the scale in the plane where the specimen is located. Hence, in order to describe the impact of the aberration in the HRTEM image plane, one needs to consider the lateral magnification $M$ which is employed to record the micrograph. The magnification $M$ is determined by the objective lens and the (magnification) setting of the projector lens system. It is assumed that the coordinates in the object plane are related to the coordinates in the image plane by a linear magnification change. Under ideal imaging conditions, an image point $w_\mathrm{o}$ in the object plane is imaged as a stigmatic image point $w_\mathrm{i}$, with $w_\mathrm{i} = -M w_\mathrm{o}$. However, if one wants to know the impact of the aberration $\Delta w_\mathrm{i}$ in terms of the resolution of the micrograph, one needs to relate the impact of the aberration to the scale of the object. For this case, the magnification $M$ can simply be ignored ($M = 1$) in the above equations and one obtains the impact of the aberration on the scale of the specimen, i.e. the impact of the aberration referred back to the specimen (see, e.g. Hawkes, 2009b). Though this is the relevant measure for the resolution of the imaging process, it does not provide information on the extent of the aberration in the detector plane.

The following example shall illustrate this distinction. Let us assume that $C_3 = 1$ mm, i.e. a typical value of the third-order spherical aberration of a conventional objective lens. The rays that should be brought to focus by the lens shall pass the aperture in $|\omega| = |\omega_\mathrm{a}| = 10$ mrad. Furthermore, we shall employ a microscope magnification in HRTEM mode of $M = 10^6$. According to Eq. (7.5), the radius of the corresponding aberration disk in the detector plane is 1 mm. However, from this we do not directly learn anything of its impact on the resolution of the imaging process. For this we need to know the impact of the aberration referred back to the specimen. Hence, ignoring $M$ in Eq. (7.5), or actually setting $M = 1$, yields the impact of $C_3$ in respect to the specimen. The radius of the aberration disk referred back to the object is then 1 nm. While the first value depends on the applied magnification, the second one is independent of the magnification and can be used to directly describe the impact of the aberration on specimen features that need to be resolved. Hence, one often uses this reduced effect, i.e. the effect of the aberration referred back to the specimen plane, in order to describe the impact of a given aberration, keeping in mind, however, that aberrations actually impact the image, which, in HRTEM, is a magnified image of the object.

In STEM, the situation is the same; the aberration coefficients are defined in the plane of the specimen. However, in STEM mode, the specimen plane is the plane where the electron beam is brought to focus and the electron probe is formed. Since this is the relevant plane where the impact of the aberrations needs to be known, the lateral magnification $M$ in Eqs. (7.5) and (7.6) can be set to $M = 1$.

Comparing Eq. (7.5) with the radius of the disk of least confusion given in Eq. (3.5) shows that the aberration figure in the Gaussian image plane is four times larger than the aberration figure in the plane where the disk of least confusion is

ABERRATION-CORRECTED IMAGING IN TRANSMISSION ELECTRON MICROSCOPY - An Introduction
© Imperial College Press
http://www.worldscibooks.com/materialsci/p703.html

located. The focal distance between the Gaussian image plane, for which Eq. (7.5) is valid, and the plane where the disk of least confusion is located, measures

$$C_{1\,\mathrm{DLC}} = -\frac{3}{4} M_{\mathrm{L}} C_3 |\omega|^2, \tag{7.7}$$

where $M_{\mathrm{L}}$ is the longitudinal magnification (see Eq. (6.97)).

The negative defocus offset $C_{1\,\mathrm{DLC}}$ indicates that the plane containing the disk of least confusion is in front of the Gaussian image plane. Comparing the defocus offset $C_{1\,\mathrm{DLC}}$ with the Scherzer focus given in Eq. (2.21) essentially shows that working at Scherzer focus implies adjusting the defocus in such a way that the disk of least confusion is moved towards the Gaussian image plane. In this way, the impact of $C_3$ on the imaging process can be minimized. This is indeed an alternative way of interpreting the Scherzer focus and the defocus associated with the Scherzer incoherent condition given in Eq. (3.9).

Hence, the fact that the disk of least confusion is located in front of the Gaussian image plane is the consequence that the spherical aberrations causes rays of finite $\omega$ to cross the optical axis in front of the Gaussian image plane.

7.4.0.2 *Coma*

Coma is the second of the symmetry, permitted geometrical aberrations of a round lens, which we introduce here. As the name of the aberration suggests, the aberration figure caused by coma resembles that of a comet: a comet-like tail emerges from a sharp distinct point. This distinct point reflects the location of the Gaussian image point. Hence, in the presence of coma, each object point is imaged into a specific coma figure, as illustrated schematically in Fig. 7.4. A set of rays emerging from an object point $w_{\mathrm{o}}$, which passes the aperture in a given angle $|\omega|$, leads to a circle in the image plane. The radius $r$ of the circle is given by $r = |MB_{3\,1} w_{\mathrm{o}}|\omega\overline{\omega}$, where $B_{3\,1}$ is the coefficient of third-order coma and $M$ is the lateral magnification.

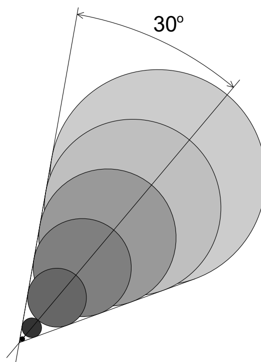


Fig. 7.4 Coma aberration figure.

ABERRATION-CORRECTED IMAGING IN TRANSMISSION ELECTRON MICROSCOPY - An Introduction
© Imperial College Press
http://www.worldscibooks.com/materialsci/p703.html

The center of the circle formed by rays that pass the aperture in $|\omega|$ is displaced from the Gaussian image point by the length $l$, which is twice the radius of the circle, i.e. $l = 2 \cdot |MB_{3\,1}w_{\mathrm{o}}|\omega\overline{\omega}$. For the whole range of $|\omega|$-values as determined by the opening of the aperture, a continuous series of circles is formed whose radii and distances to the Gaussian image point increase with increasing $|\omega|$. The individual circles lie on a line. The envelope of the aberration figure forms an angle of 60° limited by the perimeter of the largest circle reflecting the largest $|\omega|$, which is determined by the diameter of the aperture opening.

While in light optics, coma can be described by one (real) aberration coefficient $B_{3\,1}$, this is not generally possible in electron optics. In the presence of a magnetic field, which causes an electron to follow a helical trajectory defined by the Larmor rotation, coma in magnetic electron lenses comprises two contributions; *radial* (or *isotropic*) coma and *azimuthal* (or *anisotropic*) coma. Hence, in general two coefficients are necessary to describe coma of a round magnetic electron lens. However, here the complex expression of the geometrical ray parameters allows us to describe the aberration coefficients by one complex quantity. The radial and azimuthal coma is written as one complex coefficient $B_{3\,1}$, whose real part $\Re(B_{3\,1})$ reflects the radial coma and whose imaginary part $\Im(B_{3\,1})$ describes the azimuthal coma.

Figure 7.5 schematically illustrates the effects of radial coma (a), azimuthal coma (b) and a combination of radial and azimuthal coma (b) of discrete object points imaged onto the Gaussian image plane $(x_{\mathrm{i}}, y_{\mathrm{i}})$. Each object point $w_{\mathrm{o}}$ is imaged into a coma figure. The size, or the length of the coma figure, increases with increasing $|w_{\mathrm{o}}|$. Radial coma leads to coma figures which are radially aligned, whereas azimuthal coma leads to coma figures which are aligned tangentially along rings whose center is the center of the Gaussian image plane. The combination of the two leads to coma figures which are in intermediate orientation. This is the

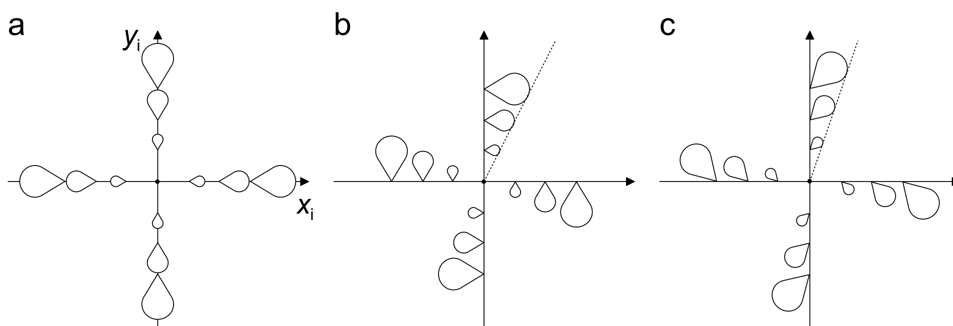


Fig. 7.5 Off-axial coma $B_{3\,1}$. (**a**) Radial coma $\Re(B_{3\,1})$, (**b**) anisotropic or azimuthal coma $\Im(B_{3\,1})$, (**c**) combination of radial and anisotropic coma. As indicated by the dotted lines, the effect of $B_{3\,1}$ vanishes for $w_{\mathrm{i}} = x_{\mathrm{i}} + \mathrm{i}y_{\mathrm{i}} \to 0$. Hence, in the center of the object plane, there is a stigmatic image point.

ABERRATION-CORRECTED IMAGING IN TRANSMISSION ELECTRON MICROSCOPY - An Introduction
© Imperial College Press
http://www.worldscibooks.com/materialsci/p703.html

general case of a magnetic lens, which has a real and imaginary coma component in $B_{3\,1}$. In the absence of magnetic fields, i.e. for pure electrostatic lenses, the azimuthal component vanishes such that $\Im(B_{3\,1}) = 0$. Hence, a purely electrostatic lens behaves like a light optical lens which shows only radial coma.

In analogy to Eq. (7.5), the image aberration $\Delta w_{\mathrm{i}}$ associated with coma $B_{3\,1}$ can be expressed as[6]

$$\Delta w_{\mathrm{i}} = -M\left[2B_{3\,1}w_{\mathrm{o}}\omega\overline{\omega} + \overline{B}_{3\,1}\overline{w}_{\mathrm{o}}\omega^2\right], \tag{7.8}$$

where $\overline{B}_{3\,1}$ indicates the complex conjugate of $B_{3\,1}$.

Comparing spherical aberration $C_3$ with coma $B_{3\,1}$ reveals a fundamental difference (see, e.g. Figs. 7.3 and 7.5). While the impact of $C_3$ depends solely on the geometrical ray parameter $\omega$ in the aperture plane (see Eq. (7.5)), Eq. (7.8) shows that the effect of coma $B_{3\,1}$ also depends on the location $w_{\mathrm{o}}$ of the object point. This simply means that coma $B_{3\,1}$ causes each object point $w_{\mathrm{o}}$ to be imaged differently. Most importantly, the effect of $B_{3\,1}$ vanishes if $|w_{\mathrm{o}}| \to 0$. Hence, while the effect of $C_3$ affects all image points equally, coma $B_{3\,1}$ affects only off-axial object points. Coma $B_{3\,1}$ is thus an off-axial aberration which impairs only object points that are not in the immediate neighborhood of the optical axis. Furthermore, the impact of coma increases linearly with $|w_{\mathrm{o}}|$. This is indicated by the dashed line in Fig. 7.5. The sum of the power of the ray parameters that describe the impact of coma in the image plane is three (see Eq. (7.8)). Therefore, coma $B_{3\,1}$ is a third-order aberration which is expressed by the first numerical subscript. Moreover, since coma increases linearly with $w_{\mathrm{o}}$, the second numerical subscript is equal one, indicating that $B_{3\,1}$ is an off-axial aberration that depends linearly on $w_{\mathrm{o}}$.

#### 7.4.0.3 *Field astigmatism and field curvature*

Astigmatism, or a bit more specifically, twofold astigmatism, is the most common correctable aberration in high-resolution electron microscopy. The kind of twofold astigmatism which is corrected to obtain and optimize atomic-resolution micrographs, however, is not the *field* astigmatism which is subject of this subsection. Nonetheless, if we consider the image of a single object point $w_{\mathrm{o}}$, the effect of field astigmatism, which as an off-axial aberration is denoted by $A_{3\,2}$, is equivalent to the effect of the common twofold astigmatism which is an *axial* aberration denoted by $A_1$. Furthermore, while field astigmatism is a symmetry-permitted aberration of a round electromagnetic lens, twofold axial astigmatism is a parasitic aberration which is caused by deviations of the electromagnetic field from an ideal rotational symmetry. Still, if we consider a single object point ($w_{\mathrm{o}} \neq 0$) and not a finite field of view, the effect of field astigmatism and axial astigmatism is conceptually comparable.

[6] We employ the notation of the aberration coefficients according to Pöhner and Rose (1974), which was also adopted by Typke and Dierksen (1995). However, we include a factor 1/3 in $B_{3\,1}$ to have the magnitude of $B_{3\,1}$ in agreement with Rose (2009a).

ABERRATION-CORRECTED IMAGING IN TRANSMISSION ELECTRON MICROSCOPY - An Introduction
© Imperial College Press
http://www.worldscibooks.com/materialsci/p703.html

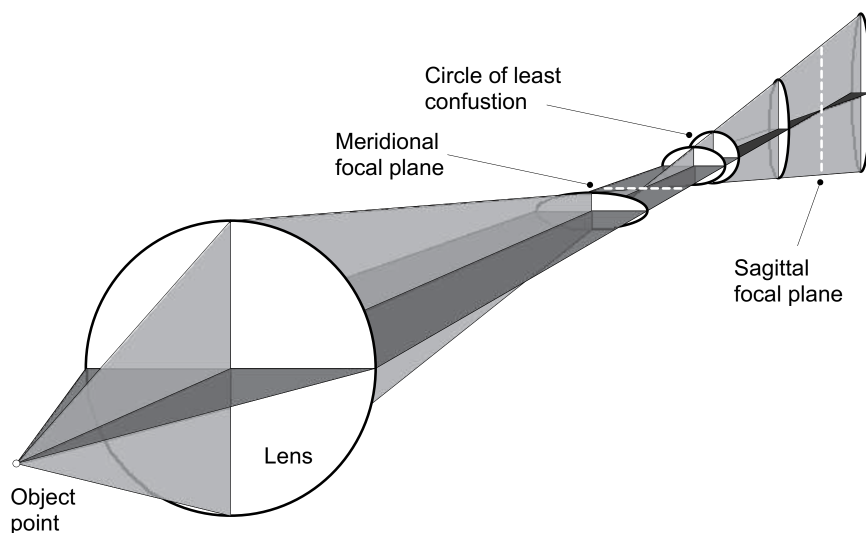


Fig. 7.6 Twofold astigmatism.

Figure 7.6 schematically illustrates the effect of twofold astigmatism on the image formation of a single object point. Electron trajectories emerge radially from the object point and enter the field of the lens, which is illustrated as a single plane corresponding to the aperture plane as well. The important point about astigmatism is that the focusing power of the lens depends on the azimuthal angle. For the case of twofold astigmatism, the focusing power is different in two orthogonal directions. This essentially means that rays described by the aperture coordinate $\omega = \theta_x + \mathrm{i}0$ are differently focused compared with rays which have the aperture coordinate $\omega = 0 + \mathrm{i}\theta_y$ (see Fig. 7.6). Hence, there is not a single focal point which would correspond to a stigmatic image. Instead, there are two orthogonal line foci, which lie in the *sagittal* focal plane and in the *tangential* or *meridional* focal plane, respectively. In Fig. 7.6, the meridional line focus is in front of the sagittal line focus. This, however, can be reversed if the focusing power of the lens is opposite to the illustration in Fig. 7.6. The Gaussian image plane lies between the meridional and sagittal focal planes. For an arbitrary coordinate along the optical path of the pencil, the image of the object point is an ellipse. For one particular position, the ellipse degenerates to a circle. In the sagittal and in the meridional plane, the ellipse degenerates to a line. Though the round beam between sagittal and meridional focal planes is not a stigmatic image point, in the presence of twofold astigmatism this is the best image that can be obtained from the object point. As in the presence of spherical aberration $C_3$, this circle is called the circle of least confusion. Hence, though a stigmatic image point is not feasible in the presence of twofold astigmatism, for a suitable focus setting it is still possible to have an object point imaged as a circular disk.

ABERRATION-CORRECTED IMAGING IN TRANSMISSION ELECTRON MICROSCOPY - An Introduction
© Imperial College Press
http://www.worldscibooks.com/materialsci/p703.html

In the presence of *field astigmatism* $A_{3\,2}$, Fig. 7.6 in principle still applies, provided, however, that only one single object point is considered, and that this object point is not identical to the point on the optical axis, i.e. $w_\mathrm{o} \neq 0$. Yet, the situation is more complex. In the presence of field astigmatism, the twofold astigmatism increases quadratically with its off-axial distance. Therefore, in order to clearly differentiate twofold field astigmatism $A_{3\,2}$, which is an off-axial aberration, from the twofold axial astigmatism $A_1$, $A_{3\,2}$ is sometimes called Seidel astigmatism or Seidelian astigmatism, referring to the fact that it is one of the Seidel aberrations, whereas twofold axial astigmatism $A_1$ is a parasitic aberration of a round lens.

The image aberration $\Delta w_\mathrm{i}$ associated with field astigmatism can be expressed as (see, e.g. Rose, 2009a)

$$\Delta w_\mathrm{i} = -MA_{3\,2}\overline{\omega}w_\mathrm{o}^2. \tag{7.9}$$

Equation (7.9) reveals that the impact of $A_{3\,2}$ increases quadratically with the off-axial distance $|w_\mathrm{o}|$. Furthermore, because field astigmatism is a third-order aberration which quadratically increases with the off-axial distance of the object point, two numerical subscripts are employed in $A_{3\,2}$.

In fact, the appearance of field astigmatism is intuitively understandable if we consider the lens field observed from a selected object point in front of the lens. For an object point on the optical axis, the field of the lens looks rotationally symmetric. No astigmatism is thus expected for an axial point. However, an off-axial object point sees the rotationally symmetric field from an angle, and what looks from the optical axis to be a circle appears as an ellipse for the off-axial position. The off-axial point thus experiences an ‘elliptical’ lens field, which, according to Fig. 7.6, explains the resulting astigmatic image formation.

Similar to the case of coma $B_{3\,1}$, due to the Larmor rotation in the presence of a magnetic field, field astigmatism can have two components; a radial component and an azimuthal component. This circumstance can be accounted for by employing a complex aberration coefficient $A_{3\,2}$, whose real part reflects the radial contribution and whose imaginary part corresponds to the azimuthal astigmatism caused by the magnetic field contribution.

In addition to field astigmatism, there is another aberration present whose impact increases quadratically with the off-axial distance of an object point. *Field curvature* (or image curvature) essentially causes the defocus to vary across the field of view. The corresponding image aberration can be described by

$$\Delta w_\mathrm{i} = -MF_{3\,2}\omega w_\mathrm{o}\overline{w}_\mathrm{o}. \tag{7.10}$$

Equation (7.10) reveals that field curvature is a third-order aberration similar to field astigmatism. This is expressed by the first numerical subscript in $F_{3\,2}$. Furthermore, as the impact of field curvature increases quadratically with the off-axial distance of the object point, the second numerical subscript is 2. The aberration coefficient $F_{3\,2}$ is real, i.e. it does not have an imaginary part.

ABERRATION-CORRECTED IMAGING IN TRANSMISSION ELECTRON MICROSCOPY - An Introduction
© Imperial College Press
http://www.worldscibooks.com/materialsci/p703.html

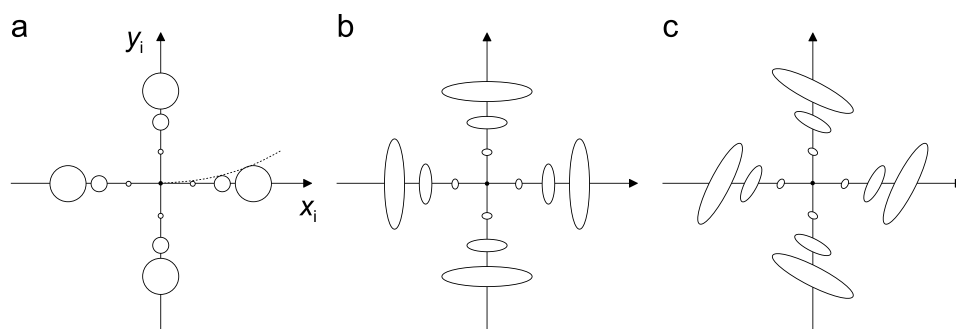


Fig. 7.7 Field curvature and field astigmatism. (**a**) Image aberration caused by field curvature, (**b**) the effect of radial field-astigmatism and image curvature, and (**c**) the combined effect of field curvature and radial and azimuthal field-astigmatism. The dotted line indicates that for $|w_i| = |x_i + iy_i| \to 0$, the effect of field curvature and field astigmatism vanishes.

By changing the defocus across the field of view, field curvature, as its name suggests, essentially causes the stigmatic image plane to bend. Hence, the effect of field curvature vanishes if the image is recorded on a suitably curved detector plane. However, for a plane detector placed in the Gaussian image plane, an object point $P_1$, which is located in a distance $|w_o|$ from the optical axis, is imaged as a disk reflecting that it is out of focus. Furthermore, an object point $P_2$, which is located in a distance $2|w_o|$ from the optical axis, i.e. twice the off-axial distance of $P_1$, is imaged as a disk which is four times larger than the disk corresponding to the object point $P_1$. This is illustrated in Fig. 7.7a. For vanishing off-axial distance, i.e. if $|w_o| \to 0$, the corresponding object point is imaged unaffected from field curvature and field astigmatism. This is clearly different from the effect of spherical aberration, which affects all object points equally (see Fig. 7.3).

The co-presence of field astigmatism and field curvature causes the elliptical distortion of an image point to increase with increasing off-axial distance. This is illustrated for the case of radial field astigmatism in Fig. 7.7b, and for the case of a combination of radial and azimuthal field astigmatism in Fig. 7.7c.

#### 7.4.0.4 *Distortion*

All of the symmetry-permitted aberrations of a round lens that we have discussed so far, namely spherical aberration $C_3$, coma $B_{3\,1}$, field astigmatism $A_{3\,2}$ and field curvature $F_{3\,2}$, caused the image of an object point to appear as an astigmatic image point. The image points are either disks, coma figures, ellipses or combination of these figures. The effect of spherical aberration does not depend on the position of the object point, whereas for the cases of coma $B_{3\,1}$, field astigmatism $A_{3\,2}$ or field curvature $F_{3\,2}$, the image aberration increases with the off-axial distance. For these off-axial aberrations, the image aberration vanishes for an object point on the optical axis. An axial object point has a corresponding stigmatic image point.

ABERRATION-CORRECTED IMAGING IN TRANSMISSION ELECTRON MICROSCOPY - An Introduction
© Imperial College Press
http://www.worldscibooks.com/materialsci/p703.html

*Image distortion*, as the fifth of the symmetry-permitted aberrations of a round lens, does not affect the formation of stigmatic image points. As the name suggests, image distortion causes a given field of view to appear as a distorted image of the object. Nevertheless, each object point finds a corresponding stigmatic image point in the distorted image. The image aberration associated with image distortion can be expressed as

$$\Delta w_{\mathrm{i}} = -MD_{3\,3}\, w_{\mathrm{o}}^{2}\overline{w}_{\mathrm{o}}. \tag{7.11}$$

This relation shows that image distortion is a third-order aberration whose impact increases with the third order of the geometrical ray parameter in the object plane $w_{\mathrm{o}}$. On the other hand, the impact of image distortion does not depend on the ray parameter $\omega$ in the aperture plane. This explains why each object point finds a stigmatic image point as a counterpart, regardless of the resolution of the instrument.

Let us consider object points arranged on a square lattice, as illustrated by the dashed mesh in Fig. 7.8. *Radial* or *isotropic* image distortion cause the image of this mesh to appear either as a pincushion-type distorted mesh or as a barrel-type distorted mesh. These two types of distortions are illustrated in Figs. 7.8a and 7.8b, respectively. Pincushion and barrel distortions are the types of distortions that are feasible in round light optical lenses, as well as in purely electrostatic electron lenses. If, however, a magnetic field is present, which forces the electrons to follow helical trajectories, *spiral* or *azimuthal* distortion becomes feasible, too. This is illustrated in Fig. 7.8c. Hence, magnetic electron lenses generally lead to image distortions which are combinations of azimuthal distortion with either the barrel or pincushion distortion (see Fig. 7.8).

Similar to the complex aberration coefficients described above, the barrel or pincushion distortion is described by the real part of $D_{3\,3}$, and the spiral or azimuthal distortion is reflected in the imaginary part of $D_{3\,3}$.

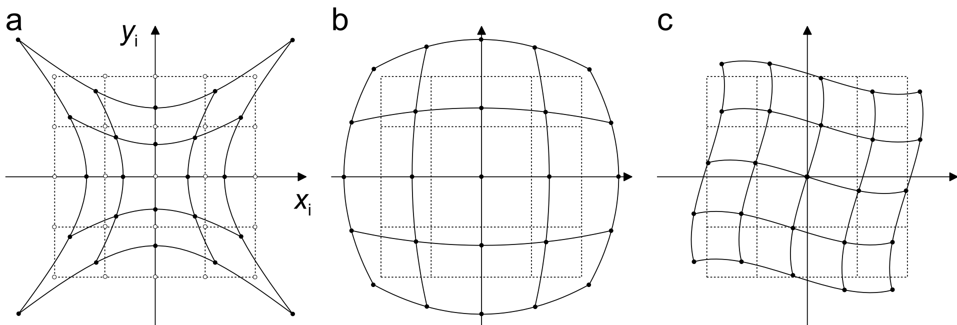


Fig. 7.8 Image distortions. The mesh indicated by the dashed lines represents the undistorted image. (**a**) Pincushion distortion, (**b**) barrel distortion and (**c**) spiral or azimuthal distortion.

ABERRATION-CORRECTED IMAGING IN TRANSMISSION ELECTRON MICROSCOPY - An Introduction
© Imperial College Press
http://www.worldscibooks.com/materialsci/p703.html

It has to be emphasized that the contribution of the objective lens to the total image distortion in HRTEM imaging is small. The reason for this is simple: the object area is small. This, however, is not necessarily the case for the projector lenses behind the objective lens. The projector lenses stepwise increase the magnification of the transferred object. Hence, the size of the object that needs to be transferred and further magnified increases within the projector lens system. As a consequence, if image distortions are observable, they are caused mostly by the projector lenses.

#### 7.4.0.5 *Summary*

Spherical aberration $C_3$, coma $B_{3\,1}$, field astigmatism $A_{3\,2}$, field curvature $F_{3\,2}$, and image distortion $D_{3\,3}$ — these are the so-called Seidel aberrations, i.e. the symmetry-permitted geometrical third-order aberrations of a round lens. This is true for the case of light optical lenses (see, e.g. Born and Wolf, 2001) as well as for the round lenses used in electron optics (see, e.g. Hawkes and Kasper, 1989a). In light optics, and for the case of purely electrostatic electron lenses, all five aberrations are describable by real coefficients. Hence, five independent numerical values are needed to describe the aberrations of a round lens. However, in the case of magnetic electron lenses, coma $B_{3\,1}$, field astigmatism $A_{3\,2}$ and image distortion $D_{3\,3}$ are described by complex values of non-vanishing imaginary parts. Hence, in electron optics one generally ends up with eight independent numerical aberration coefficients. Table 7.1 summarizes the Seidel aberrations and their respective image aberrations.

An important aspect of these aberrations concerns their off-axial dependence and their relevance for high-resolution imaging. While the impact of the off-axial aberrations, namely coma $B_{3\,1}$, field astigmatism $A_{3\,2}$, field curvature $A_{3\,2}$ and image distortion $D_{3\,3}$, vanishes for object points located on the optical axis (see Figs. 7.5, 7.7 and 7.8), the only geometrical aberration which impacts the image of object points on the optical axis is the spherical aberration $C_3$ (see Fig. 7.3). We recall the isoplanatic approximation, which simplifies the imaging process by assuming that the entire field of view (at high magnification) experiences the same phase contrast transfer function or, alternatively, the same electron probe, which

Table 7.1 Seidel aberrations; the symmetry-permitted geometrical third-order aberrations of a round lens.

| Aberration | Symbol | Value | Image aberration $\Delta w_{\rm i}$ |
|---|---|---|---|
| Third-order spherical aberration | $C_3$ | real | $-MC_3\overline{\omega}\omega^2$ |
| Coma | $B_{3\,1}$ | complex | $-M\left[2B_{3\,1}{\rm w_o}\omega\overline{\omega} + \bar{B}_{3\,1}\overline{\rm w}_{\rm o}\omega^2\right]$ |
| Field astigmatism | $A_{3\,2}$ | complex | $-MA_{3\,2}\overline{\omega}{\rm w_o^2}$ |
| Field curvature | $F_{3\,2}$ | real | $-MF_{3\,2}\omega{\rm w_o}\overline{\rm w}_{\rm o}$ |
| Image distortion | $D_{3\,3}$ | complex | $-MD_{3\,3}\,{\rm w_o^2}\overline{\rm w}_{\rm o}$ |

ABERRATION-CORRECTED IMAGING IN TRANSMISSION ELECTRON MICROSCOPY - An Introduction
© Imperial College Press
http://www.worldscibooks.com/materialsci/p703.html

in fact is valid only for the axial point. Considering that all off-axial aberrations vanish on the optical axis, it is indeed solely the spherical aberration $C_3$ which remains effective for the imaging characteristics of near-axial object points. It is for this reason why the spherical aberration is said to be the limiting aberration in electron microscopy. Compared to the impact of the spherical aberration, the effects of coma, field astigmatism, field curvature and image distortion are negligible within the isoplanatic approximation.

Although it is valuable for high-resolution electron microscopy, the isoplanatic approximation is not necessarily suitable in other domains that employ round electron lenses. For electron optical devices other than transmission electron microscopes, it is not necessarily the spherical aberration which is the most troublesome aberration. In electron lithography, field curvature and field astigmatism are the most disturbing aberrations. These aberrations limit the field of view, i.e. the area of the lithographic mask, and thus complicate processing of large areas.

Besides the fact that the object area is small in transmission electron microscopy, the impact of off-axial aberrations can be minimized to some extent. For instance, it can be shown that by setting the aperture plane in HRTEM imaging to a plane, which is in between the object plane and the back focal plane, the radial coma, i.e. $\Re(B_{3\,1})$, can be annulled. The point on the optical axis in this coma-free plane is called the coma-free point (see, e.g. Rose, 2009a, Typke and Dierksen, 1995). The coma-free point is roughly in a distance $2/3f$, where $f$ is the focal distance of the lens. However, though this allows for minimizing the effect of radial coma, its azimuthal counterpart, which is unavoidable in the presence of a magnetic field, remains unaffected by this procedure. Hence, the azimuthal coma, i.e. $\Im(B_{3\,1})$, is invariant. Still, by placing the pivot point of the beam in a scanning transmission electron microscope in the coma-free point, the scanning beam does not produce any radial coma which would reduce the achievable resolution for object points that are in a finite distance from the optical axis.

A strategy to minimize the impact of the azimuthal components of coma $B_{3\,1}$, field astigmatism $A_{3\,2}$ and in particular of image distortion $D_{3\,3}$, is based on the fact that these azimuthal aberrations are caused by the Larmor rotation. As discussed in Chapter 6, changing the polarity of a magnetic lens does not affect the focusing property of the lens, however, it reverses the Larmor rotation and as a result it also reverses the azimuthal image aberrations (see, e.g. Glaser, 1952). Transferring an electron beam through a series of round electron lenses, as in the projector system of an electron microscope, it is advantageous to alternate the polarity of consecutive lenses. This minimizes the overall azimuthal image aberrations.

Though the impact of off-axial symmetry permitted aberrations is small or can be minimized to some extent, the spherical aberration, which has the order of magnitude of the focal length of a lens, remains, affecting the imaging characteristics of a (scanning) transmission electron microscope. Furthermore, the symmetry permitted aberrations are not the only aberrations which are of relevance in real

ABERRATION-CORRECTED IMAGING IN TRANSMISSION ELECTRON MICROSCOPY - An Introduction
© Imperial College Press
http://www.worldscibooks.com/materialsci/p703.html

electron optical systems. Due to mechanical imperfections, the ideal symmetry can never be fully established in a real electron optical unit. This leads to the appearance of geometrical (and chromatic) aberrations which one would not expect under ideal circumstances. Hence, even a round electron lens can lead to a larger variety of geometrical aberrations than the ones discussed above. Since the effect of off-axial aberrations vanishes for object points on the axis, the relevant parasitic aberrations are the ones which do not vanish for object points on the optical axis. These aberrations are the axial or aperture aberrations. They are also effective within the isoplanatic approximation. For the case of a round electron lens, the only symmetry-permitted third-order aberration, which is an axial aberration, is spherical aberration. Even in the simple case of rotationally symmetric devices, the non-ideality of a round electron lens leads to more axial aberrations, such as, for example, twofold axial astigmatism $A_1$ or axial coma $B_2$.

Moreover, due to the fact that aberration correctors employ multi-pole lenses (see Chapter 8), the variety of residual geometrical aberrations in such electron microscopes can be significantly larger than for conventional electron microscopes. Deciding whether a certain aberration is caused by a slightly misaligned multi-pole lens or by a mechanical imperfection of an optical element is in general not a trivial problem to solve. Hence, in the foregoing of this chapter, we do not strictly distinguish between parasitic aberrations and permitted geometrical aberrations. However, we would like to point out that this distinction is of fundamental importance in the discussion of the performance of an optical element of a given symmetry (see, e.g. Haider *et al.*, 1982), and also in the design of aberration correctors, where in fact permitted geometrical aberrations of multi-pole lenses are used to balance the intrinsic aberration of the round objective lens.

## 7.5 Wave Surface, Aberration Function and Image Aberrations

So far, we have been dealing with effects of the aberrations in the image plane, i.e. with image aberrations $\Delta w_{\mathrm{i}}$. For TEM imaging, this plane is the detector plane and for STEM, it is the specimen plane where an image of the demagnified electron source is formed. Describing the effects of the aberrations in the image plane is one way to deal with aberrations. Another approach, which is based on Fig. 5.13, is to explain the aberrations in terms of curved wave surfaces. In this section, we would like to make the connection between (axial) image aberrations and the concept of the geometrical wave front which we introduced in Chapter 5.

We have seen in Chapter 5 that the point eikonal $S$ is a function which describes the geometrical behavior of a pencil of electron trajectories (see Fig. 5.10). The point eikonal $S$ depends on two points, such that $S = S(P_0, P)$. These points can be any two points in space. According to the principle of Maupertius (or the principle of reduced action) (see Eq. (5.50)), rays are defined by $S \to$ extremum. The eikonal $S$ can be understood as a path length of a trajectory connecting point $P_0$ with $P$.

ABERRATION-CORRECTED IMAGING IN TRANSMISSION ELECTRON MICROSCOPY - An Introduction
© Imperial College Press
http://www.worldscibooks.com/materialsci/p703.html

Though we can identify $S$ with a path *length*, we did not draw any attention to its physical dimension. In the definition of $S$ in Eq. (5.27) and similarly in the principle of Maupertius in Eq. (5.50), the unity of $S$ is given by the unity of the (canonical) momentum multiplied by the unity of a distance. Hence, in order to have the dimension of $S$ equal to a distance we must in principle normalize $S$ by the momentum $2\pi\hbar k_0$ of the incident electrons where $k_0$ is equal to the modulus of the wave vector of the incident electrons, i.e. $k_0 = 1/\lambda$. With this formal change, $S$ has the required dimension, i.e. $S$ shall describe the path length of an electron trajectory between two points. In the foregoing text we shall identify $S$ as being normalized such that its dimension corresponds to a distance.

Besides the interpretation of $S$ as a path length, we also explained that the set of points determined by

$$S(P_0, P) = \text{constant}$$

defines a surface which we called the *geometrical wave surface* (see Eq. (5.27)). Furthermore, Figs. 5.12 and 5.13, summarized in Fig. 7.9, illustrate that for an ideal imaging system which images a point of the object space into a stigmatic point in the image space, the geometrical wave surface has to be spherical. If deviations from a spherical wave surface occur, an object point is not imaged into a stigmatic image point (see Fig. 7.9b). An astigmatic image is thus the result of a deformed wave surface.

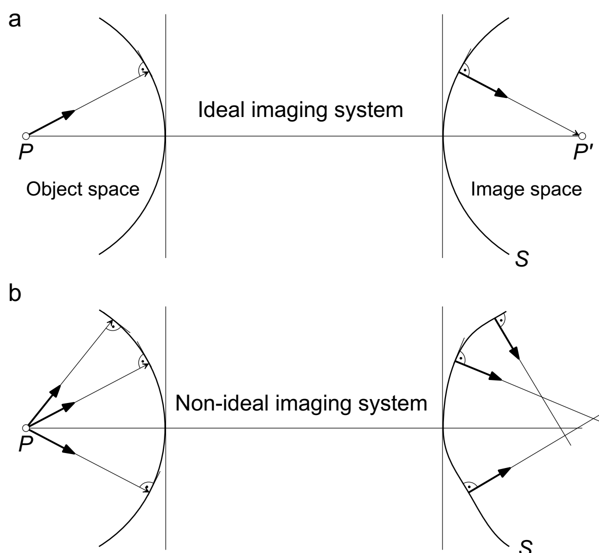


Fig. 7.9 Wave fronts. (**a**) An ideal imaging system translates a spherical wave surface into another spherical wave surface which forms a stigmatic image point $P'$ of the object point $P$. (**b**) For a non-ideal imaging system, the wave surface in the image space is not spherical. The formation of a stigmatic image point is not possible.

ABERRATION-CORRECTED IMAGING IN TRANSMISSION ELECTRON MICROSCOPY - An Introduction
© Imperial College Press
http://www.worldscibooks.com/materialsci/p703.html

### 7.5.1 *HRTEM and STEM*

From this rather conceptional argument about the imaging properties of an ideal and a non-ideal imaging system, we have to identify where, i.e. in which plane of the electron microscope, the geometrical wave surfaces are of relevance for the discussion of the imaging properties of the microscope.

In HRTEM mode, we would like to form stigmatic images of all the points of the exit-plane wave, which is located in the object plane. The image shall be formed in the image plane where the electron detector is located. Hence, the relevant geometrical wave surfaces are behind the object plane.

A point $w_\mathrm{o}$ in the object plane, where the specimen is located, can be considered to be the source point of a pencil of rays. In the field-free space, this pencil is described by a spherical wave surface (see Fig. 7.10a). Each ray of this pencil passes the aperture plane at a different location $\omega$. Depending on the source point $w_\mathrm{o}$ and its coordinate $\omega$ in the aperture plane, i.e. depending on its geometrical ray parameters ($\omega$ and $w_\mathrm{o}$), a ray can suffer from a specific phase shift due to the presence of geometrical aberrations. The phase shifts are induced by the non-ideality of the lens whose functionality it is to focus the pencil to a single point in the image plane. For a lens free of aberrations, the spherical wave surface in front of the lens is transferred into a spherical wave surface behind the lens. A stigmatic image point $w_\mathrm{i}$ results. This is illustrated in Fig. 7.10a. However, on transferring the spherical wave surface from the object space into the image space, a non-ideal lens causes the spherical wave surface to warp. The quantity that describes the deviation from the spherical wave surface for an object point located in $w_\mathrm{o}$ that emits a ray into the aperture plane at $\omega$ is the aberration function. Because of the aberration function, which will be introduced in the following section, a point in the object plane is not imaged as a stigmatic point in the image plane. Instead, the object point is imaged as a characteristic aberration figure described by the image aberration $\Delta w_\mathrm{i}$.

In STEM mode, we would like to have a stigmatic image of the idealized point-like electron source. The image of the demagnified source shall be formed in the plane where the specimen is located. The focal point of the objective lens' pre-field defines the STEM probe. Blurring of this focal point due to geometrical or chromatic aberrations simply means that the STEM probe becomes larger. This, of course, impairs the achievable resolution. The relevant geometrical wave surface is thus in front of the specimen plane.

Although we have seen in Chapter 3 that the finite brightness prevents the formation of an infinitely small demagnified electron source, let us assume that the electron source is demagnified to a single point located in $w_\mathrm{o}$ (see Fig. 7.10b). The source point in $w_\mathrm{o}$ can be considered to emit a pencil of rays. This pencil is described by a spherical wave surface. Its angular range $\omega$ is defined by the aperture opening which provides the measure for the illumination semi-angle $\alpha$. By focusing the pencil onto the specimen plane, the pre-field of the objective lens images the

ABERRATION-CORRECTED IMAGING IN TRANSMISSION ELECTRON MICROSCOPY - An Introduction
© Imperial College Press
http://www.worldscibooks.com/materialsci/p703.html

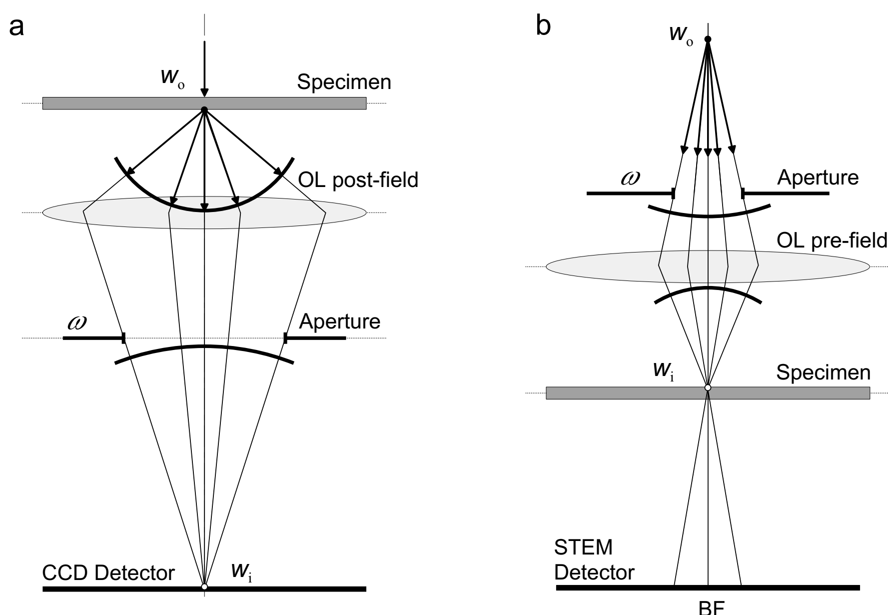


Fig. 7.10 The relevant geometrical wave surfaces in TEM and in STEM.

source point onto the specimen plane. The image of the source point in $w_o$ is the electron probe. For the ideal case of an aberration-free lens, the spherical wave surface in front of the objective lens' pre-field is transferred to a spherical wave surface behind the lens. As illustrated in Fig. 7.10b, under this idealized condition, a stigmatic image point $w_i$ results. However, geometrical aberrations of the lens cause the spherical wave surface behind the lens to curve, such that the pencil is not focused to a stigmatic image point.

According to the eikonal, the pencil of rays is fully defined by two geometrical ray parameters. Though we are essentially free in the choice of the position variables that shall describe the pencil of rays, we would like to know the wave surface in the relevant planes. In STEM mode, it is the wave surface in the front focal plane which defines the electron probe on the specimen plane. In HRTEM, it is the wave surface in the back focal plane which determines the imaging characteristics of a particular object point (see Fig. 7.10). Hence, it is common to choose the first position variable $P_0$ to be in the relevant aperture plane $\omega$ (front focal plane for STEM and back focal plane for HRTEM), and the other position $w_o$ to be in the object plane, which for STEM is the location of the (demagnified) source point and for HRTEM is the specimen plane (see Fig. 7.10). Hence, $S = S(w_o, \omega)$. The aberrations become apparent in the image plane $w_i$, which for STEM is the specimen plane and for HRTEM is the detector plane.

ABERRATION-CORRECTED IMAGING IN TRANSMISSION ELECTRON MICROSCOPY - An Introduction
© Imperial College Press
http://www.worldscibooks.com/materialsci/p703.html

### 7.5.2 *Non-ideal geometrical wave surfaces*

As pointed out above, the curvature of a wave surface $S = S(\mathrm{w_o}, \omega)$ defines the aberration in the image space. While the geometrical wave surface of an ideal imaging system is a sphere (see Fig. 7.9a), a non-ideal imaging system does not have a spherical wave surface (see Fig. 7.9b). However, provided the deviations from the spherical surface are small, we can conveniently describe the warped wave surface of a non-ideal imaging system by the superposition of the ideal spherical wave surface $S^0$ and a function $W$, which takes into account the deviation from the spherical shape. Hence, the actual wave surface $S$ is then described by $S(\mathrm{w_o}, \omega) = S^0(\mathrm{w_o}, \omega) + W(\mathrm{w_o}, \omega)$. The function $W(\mathrm{w_o}, \omega)$ is called the *aberration function*. The relation between $S$, $S^0$ and $W$ is illustrated schematically in Fig. 7.11.

### 7.5.3 *The aberration function*

The aberration function $W(\mathrm{w_o}, \omega)$ is a function that depends on the position of the object point $\mathrm{w_o}$ and on the position $\omega$ where a particular ray passes the aperture plane. Each object point $\mathrm{w_o}$ thus has its characteristic wave surface $S$, as, for example, illustrated in Fig. 7.11, which describes how this particular object point is imaged onto the image plane. This general case implies that off-axial and axial aberrations are present, such that $W$ is a real function of $\mathrm{w_o}$ and $\omega$. For the Seidel aberrations, i.e. the symmetry-permitted geometrical aberrations of a round lens, the aberration function $W$ can be written as

$$W(\mathrm{w_o}, \omega) = \Re\left\{\frac{1}{2}C_1\omega\overline{\omega} + \frac{1}{4}C_3\left(\omega\overline{\omega}\right)^2 + B_{3\,1}\omega\overline{\omega}^2\mathrm{w_o} + \frac{1}{2}F_{3\,2}\omega\overline{\omega}\mathrm{w_o}\overline{\mathrm{w}}_\mathrm{o} + \frac{1}{2}A_{3\,2}\overline{\omega}^2\mathrm{w_o^2} + D_{3\,3}\overline{\omega}\mathrm{w_o^2}\overline{\mathrm{w}}_\mathrm{o}\right\}. \tag{7.12}$$

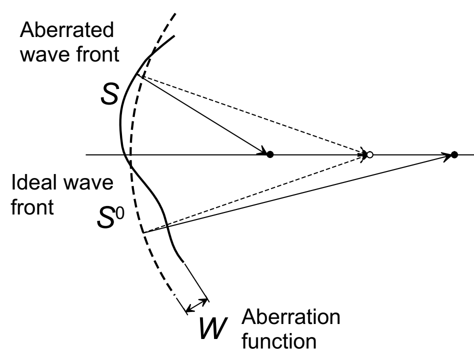


Fig. 7.11 The aberration function $W$ is the difference between the actual, i.e. the aberrated, wave front $S$ and the ideal spherical wave front $S^0$, $S = S^0 + W$.

ABERRATION-CORRECTED IMAGING IN TRANSMISSION ELECTRON MICROSCOPY - An Introduction
© Imperial College Press
http://www.worldscibooks.com/materialsci/p703.html

The aberration coefficients, which were introduced in the previous section to describe image aberrations $\Delta w_{\mathrm{i}}$, are employed here to define the curvature of the wave front in respect to the spherical reference wave front. Besides the Seidel aberrations, namely spherical aberration $C_3$, coma $B_{31}$, field astigmatism $A_{32}$, field curvature $F_{32}$ and image distortion $D_{33}$, we also included a term with $C_1$ describing the adjustable defocus of the lens. Equation (7.12) thus enables us to describe the bending of the wave surface due to the Seidel aberrations of a round electromagnetic lens. For each point $w_{\mathrm{o}}$ in the object plane, which can be considered to be a source point of a pencil of rays, Eq. (7.12) describes the deviation from a spherical wave surface in the aperture plane $\omega$. Some of the aberrations in Eq. (7.12) are axial aberrations (i.e. depend only on $\omega$ but not on $w_{\mathrm{o}}$), and some, which depend on the location of the object point $w_{\mathrm{o}}$ (or $\overline{w}_{\mathrm{o}}$), are off-axial aberrations.

Since HRTEM imaging is carried out at high magnification, the object area is small. Similarly, if we work at high magnification in STEM mode, the scanned specimen area becomes small. This implies that the scan coils need to move the demagnified source image in front of the objective lens only in a very limited lateral range. Hence, regardless of HRTEM or STEM, for high-resolution imaging, the range of $w_{\mathrm{o}}$ that needs to be considered in the deviation of the imaging characteristics is small — small enough such that we can employ the isoplanatic approximation and thus neglect the dependence of $W$ on $w_{\mathrm{o}}$. Ignoring all the terms that contain $w_{\mathrm{o}}$ or $\overline{w}_{\mathrm{o}}$ in Eq. (7.12) simply means that all off-axial aberrations are neglected. Or better, under the isoplanatic approximation, $W$ is expressed for the specific case $w_{\mathrm{o}} = 0 + \mathrm{i}0$. It is assumed that $W(0 + \mathrm{i}0, \omega)$ is valid for the small range of $w_{\mathrm{o}}$ around $w_{\mathrm{o}} = 0 + \mathrm{i}0$, which defines the field of view in high-resolution imaging. In order to distinguish $W(0 + \mathrm{i}0, \omega)$ from the general geometrical aberration function $W(w_{\mathrm{o}}, \omega)$, we denote it by $\chi$, i.e. $\chi(\omega) = W(0 + \mathrm{i}0, \omega)$.

Under the isoplanatic approximation, i.e. neglecting coma $B_{31}$, field astigmatism $A_{32}$, field curvature $F_{32}$ and image distortion $D_{33}$, one ends up with the following (axial) aberration function of a round electromagnetic electron lens

$$W(w_{\mathrm{o}}, \omega) = W(0, \omega) = \chi(\omega) = \Re\left\{\frac{1}{2}C_1\omega\overline{\omega} + \frac{1}{4}C_3\left(\omega\overline{\omega}\right)^2\right\}. \tag{7.13}$$

Equation (7.13) is equivalent to the aberration function which we employed in Chapters 2 and 3 in order to describe the phase contrast transfer function in HRTEM and to include the lens effects in the derivation of the electron probe in STEM mode, respectively. However, while in the previous chapters $\chi$ was a rather abstract function missing a physical interpretation, in the context of geometrical wave surfaces, the aberration function $\chi$ (and $W$) possesses a clear physical interpretation; $\chi$ expresses the deviation of the aberrated wave surface from the spherical wave surface, as illustrated in Fig. 7.11.

Equation (7.13) describes the effect of the remaining geometrical aberrations of a rotationally symmetric imaging (or illumination) system. Provided that the field of view is sufficiently small and that the isoplanatic approximation can be employed,

ABERRATION-CORRECTED IMAGING IN TRANSMISSION ELECTRON MICROSCOPY - An Introduction
© Imperial College Press
http://www.worldscibooks.com/materialsci/p703.html

defocus $C_1$ and spherical aberration $C_3$ are the residual aberrations which need to be considered in the image formation process. Though $C_1$ can in principle be set equal zero, a finite (negative) value is of advantage in the presence of the positive $C_3$ of the objective lens. Of course, Eq. (7.13) is only valid if the effect of parasitic axial aberrations is small compared to the effect of $C_3$. This implies, for instance, that by employing a stigmator, twofold axial astigmatism, i.e. the dominant parasitic aberration of a round lens, is corrected to a precision where its residual impact can be neglected. Furthermore, the microscope is supposed to be properly aligned such that the influence of the symmetry permitted off-axial geometrical aberrations is minimized as well. If these conditions are met, the axial aberration function can be described by defocus $C_1$ and third-order spherical aberration $C_3$. Since both, $C_1$ and $C_3$, are isotropic aberrations, reducing the aberration function to the effects of $C_1$ and $C_3$ results in an isotropic information transfer in TEM mode and in a rotationally symmetric electron probe in STEM mode.

However, reducing the problem of the information transfer in HRTEM imaging as well as the formation of the electron probe to two isotropic geometrical aberrations is not necessarily correct. Prior to the successful implementation of aberration correctors into (scanning) transmission electron microscopes, it had already been recognized that Eq. (7.13) is not appropriate to describe the information transfer for *ultra*-high resolution imaging in conventional electron microscopes. Besides the correctable twofold axial astigmatism, additional anisotropic axial aberrations, such as threefold astigmatism and axial coma, would need to be considered in the image and probe formation process (see, e.g. Krivanek, 1994; Overwijk *et al.*, 1997; Stenkamp, 1998). More drastic is the situation for aberration-corrected microscopes. The aberration function given in Eq. (7.13) is simply no longer adequate. Firstly, the third-order spherical aberration $C_3$ of the objective lens is corrected by the aberration corrector. Hence, the 'dominant' geometrical aberration, i.e. $C_3$, can in principle be annulled. For this reason, it is likely that other geometrical aberrations become important. As will be shown in detail in the following chapter, aberration correctors employ multi-pole lenses. The amount of symmetry-permitted axial aberrations is larger for multi-pole lenses than it is for round lenses (see, e.g. Hawkes and Kasper, 1989a). Moreover, because of potential mechanical imperfections of multi-pole and round lenses, parasitic geometrical aberrations can arise. Of course, such aberrations can in principle also arise in conventional microscopes. However, they might be negligible for an instrument with a $C_3$ of about 1 mm. For a microscope whose $C_3$ can be set to a value which is nearly three orders of magnitude smaller than the initial value of the uncorrected lens, even small parasitic aberrations can become important. Hence, especially for the case of aberration-corrected microscopy, axial aberrations of higher order and higher symmetry need to be considered. The presence of anisotropic aberrations destroys the rotational symmetry of the transfer process in TEM imaging, as well as the rotational symmetry of the STEM probe.

ABERRATION-CORRECTED IMAGING IN TRANSMISSION ELECTRON MICROSCOPY - An Introduction
© Imperial College Press
http://www.worldscibooks.com/materialsci/p703.html

In general, there are $(n+2)/2$ axial aberrations of $n$-th order if $n$ is an even number, i.e. $n = 2m$ with $m = 0, 1, 2, 3, ...$, and $(n+3)/2$ axial aberrations of $n$-th order if $n$ is an odd number, i.e. $n = 2m+1$. However, these numbers do not reflect whether the aberrations are real (one coefficient) or complex (two coefficients). Taking this distinction into account, there are $n+2$ independent axial aberration coefficients of order $n$. This implies that the total amount of independent axial aberration coefficients for a system where axial aberrations up to an order $n$ need to be considered, is $[(n+1)(n+4)]/2$.

Considering all feasible axial aberrations up to seventh order ($n = 7$), 44 independent aberration coefficients need to be taken into account. The corresponding (axial) aberration function $\chi(\omega)$ can be expressed as

$$\begin{aligned}\chi(\omega) = \Re \Big\{ & A_0\overline{\omega} + \frac{1}{2}C_1\omega\overline{\omega} + \frac{1}{2}A_1\overline{\omega}^2 + B_2\omega^2\overline{\omega} + \frac{1}{3}A_2\overline{\omega}^3 \\ & + \frac{1}{4}C_3\left(\omega\overline{\omega}\right)^2 + S_3\omega^3\overline{\omega} + \frac{1}{4}A_3\overline{\omega}^4 \\ & + B_4\omega^3\overline{\omega}^2 + D_4\omega^4\overline{\omega} + \frac{1}{5}A_4\overline{\omega}^5 \\ & + \frac{1}{6}C_5\left(\omega\overline{\omega}\right)^3 + S_5\omega^4\overline{\omega}^2 + R_5\omega^5\overline{\omega} + \frac{1}{6}A_5\overline{\omega}^6 \\ & + B_6\omega^4\overline{\omega}^3 + D_6\omega^5\overline{\omega}^2 + F_6\omega^6\overline{\omega} + \frac{1}{7}A_6\overline{\omega}^7 \\ & + \frac{1}{8}C_7\left(\omega\overline{\omega}\right)^4 + S_7\omega^5\overline{\omega}^3 + R_7\omega^6\overline{\omega}^2 + G_7\omega^7\overline{\omega} + \frac{1}{8}A_7\overline{\omega}^8 \Big\}, \end{aligned} \qquad (7.14)$$

where the numerical subscript of each aberration indicates its order $n$. The absence of the second numerical subscript shows that the aberrations in Eq. (7.14) are all axial (or aperture) aberrations. The names and their respective symmetry are summarized in Table 7.2. An aberration $A_n$ is the $n$-th order astigmatism which has an $(n+1)$-fold symmetry, $C_n$ is the $n$-th order spherical aberration, which is an isotropic aberration (i.e. symmetry zero), $B_n$ is the $n$-th order axial coma of symmetry 1, $S_n$ is the $n$-th order star aberration with twofold symmetry, $D_n$ is the $n$-th order three-lobe aberration with threefold symmetry, $R_n$ is the $n$-th order rosette aberration of fourfold symmetry, $F_6$ is the sixth-order pentacle aberration with fivefold symmetry and $G_7$ is the chaplet aberration with sixfold symmetry. While the isotropic aberrations, i.e. defocus $C_1$ and the spherical aberrations $C_n$, are describable by a real aberration coefficient, the anisotropic aberrations are in general related to complex coefficients, which implies that their effect is described by two independent coefficients[7].

[7] Although Eq. (7.14) looks rather complex, especially the way each aberration is weighted by $\omega$ and $\overline{\omega}$, it has a systematic structure. For a given order $n$, the aberration of highest symmetry is the astigmatism $A_n$ of symmetry $N = n+1$. Its contribution to the aberration function scales with $\overline{\omega}^{(n+1)}$. An aberration of this particular symmetry appears again in the series of aberrations of order $n+2$, $n+4$ and so on (see Table 7.2). The impact of these higher-order aberrations of equal symmetry scales by $\omega^{(n+1)}(\omega\overline{\omega})^1$ for order $n+2$ and by $\overline{\omega}^{(n+1)}(\omega\overline{\omega})^2$ for order $n+4$, and

ABERRATION-CORRECTED IMAGING IN TRANSMISSION ELECTRON MICROSCOPY - An Introduction
© Imperial College Press
http://www.worldscibooks.com/materialsci/p703.html

Table 7.2 Geometrical axial aberrations.

| Aberration | Symbol | Value | Symmetry $N$ | Wave aberration $\mathcal{R}(\cdots)$ |
|---|---|---|---|---|
| Beam/Image shift | $A_0$ | complex | 1 | $A_0\overline{\omega}$ |
| Defocus | $C_1$ | real | 0 | $\frac{1}{2}C_1\omega\overline{\omega}$ |
| Twofold astigmatism | $A_1$ | complex | 2 | $\frac{1}{2}A_1\overline{\omega}^2$ |
| Second-order axial coma | $B_2$ | complex | 1 | $B_2\omega^2\overline{\omega}$ |
| Threefold astigmatism | $A_2$ | complex | 3 | $\frac{1}{3}A_2\overline{\omega}^3$ |
| Third-order spherical aberration | $C_3$ | real | 0 | $\frac{1}{4}C_3\,(\omega\overline{\omega})^2$ |
| Third-order star-aberration | $S_3$ | complex | 2 | $S_3\omega^3\overline{\omega}$ |
| Fourfold astigmatism | $A_3$ | complex | 4 | $\frac{1}{4}A_3\overline{\omega}^4$ |
| Fourth-order axial coma | $B_4$ | complex | 1 | $B_4\omega^3\overline{\omega}^2$ |
| Fourth-order three-lobe aberration | $D_4$ | complex | 3 | $D_4\omega^4\overline{\omega}$ |
| Fivefold astigmatism | $A_4$ | complex | 5 | $\frac{1}{5}A_4\overline{\omega}^5$ |
| Fifth-order spherical aberration | $C_5$ | real | 0 | $\frac{1}{6}C_5\,(\omega\overline{\omega})^3$ |
| Fifth-order star-aberration | $S_5$ | complex | 2 | $S_5\omega^4\overline{\omega}^2$ |
| Fifth-order rosette aberration | $R_5$ | complex | 4 | $R_5\omega^5\overline{\omega}$ |
| Sixfold astigmatism | $A_5$ | complex | 6 | $\frac{1}{6}A_5\overline{\omega}^6$ |
| Sixth-order axial coma | $B_6$ | complex | 1 | $B_6\omega^4\overline{\omega}^3$ |
| Sixth-order three-lobe aberration | $D_6$ | complex | 3 | $D_6\omega^5\overline{\omega}^2$ |
| Sixth-order pentacle aberration | $F_6$ | complex | 5 | $F_6\omega^6\overline{\omega}$ |
| Sevenfold astigmatism | $A_6$ | complex | 7 | $\frac{1}{7}A_6\overline{\omega}^7$ |
| Seventh-order spherical aberration | $C_7$ | real | 0 | $\frac{1}{8}C_7\,(\omega\overline{\omega})^4$ |
| Seventh-order star-aberration | $S_7$ | complex | 2 | $S_7\omega^5\overline{\omega}^3$ |
| Seventh-order rosette aberration | $R_7$ | complex | 4 | $R_7\omega^6\overline{\omega}^2$ |
| Seventh-order chaplet aberration | $G_7$ | complex | 4 | $G_7\omega^7\overline{\omega}$ |
| Eightfold astigmatism | $A_7$ | complex | 8 | $\frac{1}{8}A_7\overline{\omega}^8$ |

so on. The numerical prefactors are chosen such that the prefactors of the corresponding image aberrations are either 1 or integers, but no fractions. As an example; the second-order aberration of highest symmetry is threefold astigmatism $A_2$ whose symmetry is $N = n + 1 = 3$. Aberrations of symmetry 3 appear again in the fourth- and sixth-order aberrations (see Fig. 7.12): fourth- and sixth-order three-lobe aberration $D_4$ and $D_6$. Since the impact of $A_2$ scales with $\overline{\omega}^3$, the impact of $D_4$ scales with $\omega^3(\omega\overline{\omega})$ and the impact of $D_6$ scales with $\omega^3(\omega\overline{\omega})^2$. The factor $(\omega\overline{\omega})$ is just a radial, parabolic angular factor. With these basic rules, the entire relation given in Eq. (7.14) can in principle be derived. Yet, the numerical prefactors need to be explained by the image aberrations, which we will relate to the wave aberrations in a subsequent part of this chapter.

ABERRATION-CORRECTED IMAGING IN TRANSMISSION ELECTRON MICROSCOPY - An Introduction
© Imperial College Press
http://www.worldscibooks.com/materialsci/p703.html

The modulations of the aberrated wave surface caused by each of these aberrations are depicted in Fig. 7.12, which also reveals the symmetry of each aberration as listed in Table 7.2. Here we define the symmetry $N$ of an aberration as follows: an aberration $X_n$ has the symmetry $N$ if the distortion of the wave surface caused by the aberration is invariant by a rotation of $2\pi/N$ about the optical axis, with $N$ being the largest number for which this is fulfilled. Hence, if an aberration function $\chi$ associated by an aberration $X_n$ shows the characteristics that

$$\chi(\omega) = \chi\left(\omega \exp\left\{\frac{2\pi \mathrm{i}}{N}\right\}\right), \tag{7.15}$$

the aberration has the symmetry $N$. The symmetry $N$ associated with an aberration shall be the maximum number $N$ for which Eq. (7.15) is valid (see, e.g. Uno *et al.*, 2005). This formal definition is intuitively understandable by looking at Fig. 7.12. The symmetry $N$ is the number of times that the aberration function repeats on being rotated about the optical axis. For the case that $N \to \infty$, $X_n$ is an isotropic aberration and apparently not fully consistent, we denote the symmetry $N = 0$.

### 7.5.4 *Other notations for axial aperture aberrations*

The notation of the axial aberration coefficients we employ here is essentially based on the notation of Pöhner and Rose (1974), which is an expansion of the definition of the aberration coefficients introduced by Plies and Rose (1971). The numerical values, i.e. the prefactors of the coefficients, are however defined according to Haider *et al.* (2008b)[8]. This implies small numerical differences between the notation of Pöhner and Rose (1974) and the one employed here (Haider *et al.*, 2008b). Table 7.3 provides a comparison between the notations of Pöhner and Rose (1974) and Haider *et al.* (2008b). The notation of Haider *et al.* (2008b) is essentially used in the aberration diagnosis software of aberration-corrected STEM/TEM instruments which are equipped with hexapole-type aberration correctors.

There are other notations of the aberration coefficients in use. This, in fact, would not cause any problems as long as the aberration coefficients have the same absolute value[9]. But even this differs between different notations. For instance, depending on whether a factor of 1/3 is implicitly used in the definition of $B_2$

[8]The advantage of using the numerical prefactors according to Haider *et al.* (2008b) is that the corresponding image aberrations do not have fractions as prefactors, but solely integers.

[9]There are many notation schemes in use. We focus on the notations most frequently used in literature. The following references provide a brief overview of different notations employed in the literature and not covered in this text: Jiye and Crewe (1985); Thust *et al.* (1996); Krivanek (1994); Overwijk *et al.* (1997); Stenkamp (1998); Lupini (2001); Xiu and Gibson (2001); Sawada *et al.* (2009). The three most common notations in aberration-corrected electron microscopy are: the ones described in detail by Uhlemann and Haider (1998) and Haider *et al.* (2008b), which are employed in, e.g. Haider *et al.* (2000); Uno *et al.* (2005); Erni *et al.* (2009); Zach (2009). Secondly, the notation described in Krivanek *et al.* (2009a), which is based on Krivanek *et al.* (1999) and which is employed, for example, by Ramasse and Bleloch (2005); Krivanek *et al.* (2008a, 2009a). Thirdly, the notation used by Pöhner and Rose (1974), which is, for example, employed in Haider *et al.* (1995); Saxton (1995); Typke and Dierksen (1995); Haigh *et al.* (2009b).

ABERRATION-CORRECTED IMAGING IN TRANSMISSION ELECTRON MICROSCOPY - An Introduction
© Imperial College Press
http://www.worldscibooks.com/materialsci/p703.html

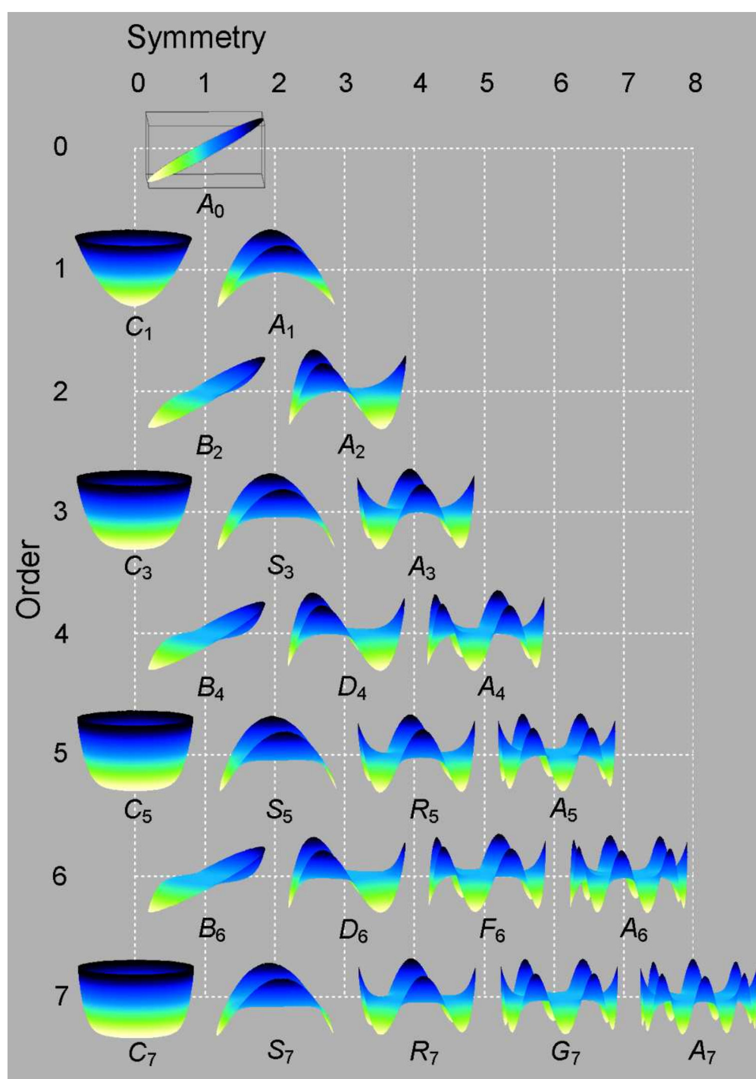


Fig. 7.12 The impact of the axial aberrations on the wave surface. Each part illustrates $\chi$ for the corresponding aberration coefficient.

(see, e.g. Eq. (7.14)) or whether the factor of 1/3 is written explicitly in the term of $B_2$, of course, changes the absolute value of the aberration coefficient and complicates the comparison between different instruments that measure the aberration coefficient based on different notations. However, the aberration function $\chi$ as given, for example, in Eq. (7.14), has to be invariant. The aberration function must be independent of the definition of the aberration coefficients and independent of the notation employed to describe a certain aberration coefficient. Furthermore, some notations do not employ complex coordinates or complex aberration coefficients but

ABERRATION-CORRECTED IMAGING IN TRANSMISSION ELECTRON MICROSCOPY - An Introduction
© Imperial College Press
http://www.worldscibooks.com/materialsci/p703.html

Table 7.3 Comparison of different notations.

| Aberration | Haider *et al.* (2008) | Krivanek *et al.* (2009) | Pöhner and Rose* (1974) |
|---|---|---|---|
| Beam/image shift | $A_0$ | $C_{0,1}$ | $A_0$ |
| Defocus | $C_1$ | $C_{1,0}$ | $C_1$ |
| Twofold astigmatism | $A_1$ | $C_{1,2}$ | $A_1$ |
| Second-order axial coma | $B_2$ | $\frac{1}{3}\,C_{2,1}$ | $\frac{1}{3}B_2$ |
| Threefold astigmatism | $A_2$ | $C_{2,3}$ | $A_2$ |
| Third-order spherical aberration | $C_3$ | $C_{3,0}$ | $C_3$ |
| Third-order star-aberration | $S_3$ | $\frac{1}{4}\,C_{3,2}$ | $\frac{1}{4}B_3$ |
| Fourfold astigmatism | $A_3$ | $C_{3,4}$ | |
| Fourth-order axial coma | $B_4$ | $\frac{1}{4}\,C_{4,1}$ | |
| Fourth-order three-lobe aberration | $D_4$ | $\frac{1}{4}\,C_{4,3}$ | |
| Fivefold astigmatism | $A_4$ | $C_{4,5}$ | |
| Fifth-order spherical aberration | $C_5$ | $C_{5,0}$ | $C_5$ |
| Fifth-order star-aberration | $S_5$ | $\frac{1}{6}\,C_{5,2}$ | $\frac{1}{6}\,B_5$ |
| Fifth-order rosette aberration | $R_5$ | $\frac{1}{6}\,C_{5,4}$ | $\frac{1}{6}\,D_5$ |
| Sixfold astigmatism | $A_5$ | $C_{5,6}$ | $A_5$ |
| Sixth-order axial coma | $B_6$ | $\frac{1}{7}\,C_{6,1}$ | |
| Sixth-order three-lobe aberration | $D_6$ | $\frac{1}{7}\,C_{6,3}$ | |
| Sixth-order pentacle aberration | $F_6$ | $\frac{1}{7}\,C_{6,5}$ | |
| Sevenfold astigmatism | $A_6$ | $C_{6,7}$ | |
| Seventh-order spherical aberration | $C_7$ | $C_{7,0}$ | |
| Seventh-order star-aberration | $S_7$ | $\frac{1}{8}\,C_{7,2}$ | |
| Seventh-order rosette aberration | $R_7$ | $\frac{1}{8}\,C_{7,4}$ | |
| Seventh-order chaplet aberration | $G_7$ | $\frac{1}{8}\,C_{7,6}$ | |
| Eightfold astigmatism | $A_7$ | $C_{7,8}$ | |

(*)Though fourth-order aberrations are not considered, the notation of Pöhner and Rose (1974) is equivalent to the notation for the axial aberration coefficients employed by Typke and Dierksen (1995) and Saxton (1995).

are, for instance, related to a cylindrical coordinate system, where an aberration is then described by an absolute value and an azimuth angle (see, for example, the comparison in Typke and Dierksen, 1995). Still, even for such definitions, the aberration function $\chi$ needs to be invariant — invariant in respect to the coordinate system chosen and the notation of the aberration coefficients. Hence, comparing

ABERRATION-CORRECTED IMAGING IN TRANSMISSION ELECTRON MICROSCOPY - An Introduction
© Imperial College Press
http://www.worldscibooks.com/materialsci/p703.html

the wave aberration function $\chi$ in different notations provides a mean of comparing different notations.

Besides the notation of Haider *et al.* (2008b) which is employed here, another often-used notation for aberration coefficients is outlined by Krivanek *et al.* (1999). With a slight modification, this notation is employed and described by Krivanek *et al.* (2008b) and Krivanek *et al.* (2009a)[10]. In the notation of Krivanek *et al.* (2009a), each aberration coefficient is denoted by $C_{n,N}$. The first numerical subscript $n$ denotes the order $n$ of the aberration, while the second numerical subscript $N$ denotes its symmetry $N$. The order $n$ and the symmetry $N$ are in agreement with the definition introduced above. While aberration coefficients with $N > 0$ can be described by two independent coefficients $C_{n,N,a}$ and $C_{n,N,b}$ (Krivanek *et al.*, 2009a), they can be equally well be described as complex numbers such that $C_{n,N} = C_{n,N,a} + \mathrm{i}C_{n,N,b}$ (Hawkes, 2009b). Because the subscripts of the coefficients make it immediately apparent what the nature (order and symmetry) of the aberration is, the notation according to Krivanek *et al.* (2009a) is particularly useful in deriving combination aberrations which arise through the superposition of two or more geometrical aberrations. However, the notation according to Haider *et al.* (2008b) needs only one numerical subscript and describes the symmetry of the aberration by the (though randomly chosen) capital letter. Employing complex aberration coefficients ($C_{n,N} = C_{n,N,a} + \mathrm{i}C_{n,N,b}$) and complex coordinates, the aberration function $\chi(\omega)$ can be expressed in the notation of Krivanek *et al.* (2009a) as

$$\begin{aligned}\chi(\omega) = \Re\Big\{ & C_{0,1}\overline{\omega} + \frac{1}{2}C_{1}\omega\overline{\omega} + \frac{1}{2}C_{1,2}\overline{\omega}^2 + \frac{1}{3}\overline{C}_{2,1}\omega^2\overline{\omega} + \frac{1}{3}C_{2,3}\overline{\omega}^3 \\ & + \frac{1}{4}C_{3,0}\left(\omega\overline{\omega}\right)^2 + \frac{1}{4}\overline{C}_{3,2}\omega^3\overline{\omega} + \frac{1}{4}C_{3,4}\overline{\omega}^4 \\ & + \frac{1}{5}\overline{C}_{4,1}\omega^3\overline{\omega}^2 + \frac{1}{5}\overline{C}_{4,3}\omega^4\overline{\omega} + \frac{1}{5}C_{4,5}\overline{\omega}^5 \\ & + \frac{1}{6}C_{5,0}\left(\omega\overline{\omega}\right)^3 + \frac{1}{6}\overline{C}_{5,2}\omega^4\overline{\omega}^2 + \frac{1}{6}\overline{C}_{5,4}\omega^5\overline{\omega} + \frac{1}{6}C_{5,6}\overline{\omega}^6 \\ & + \frac{1}{7}\overline{C}_{6,1}\omega^4\overline{\omega}^3 + \frac{1}{7}\overline{C}_{6,3}\omega^5\overline{\omega}^2 + \frac{1}{7}\overline{C}_{6,5}\omega^5\overline{\omega} + \frac{1}{7}C_{6,7}\overline{\omega}^7 \\ & + \frac{1}{8}C_{7,0}\left(\omega\overline{\omega}\right)^4 + \frac{1}{8}\overline{C}_{7,2}\omega^5\overline{\omega}^3 + \frac{1}{8}\overline{C}_{7,4}\omega^6\overline{\omega}^2 + \frac{1}{8}\overline{C}_{7,6}\omega^7\overline{\omega} + \frac{1}{8}C_{7,8}\overline{\omega}^8 \Big\}, \end{aligned} \quad (7.16)$$

where the bar in $\overline{C}_{n,N}$ denotes the complex conjugate of $C_{n,N}$.

In any case, whatever definition for the aberration coefficients is employed, the basic physical concept does not change. The aberration coefficients describe the curvature of an aberrated wave surface in respect to the ideal spherical one. Still, some boundary conditions have to be met; the number of independent aberration

[10] The notation introduced by Krivanek *et al.* (1999) has been further developed such that $C_{n,m}$ in Krivanek *et al.* (2008b) and Krivanek *et al.* (2009a) is equal to $C_{m,n}$ of Krivanek *et al.* (1999), i.e. the subscripts are interchanged.

ABERRATION-CORRECTED IMAGING IN TRANSMISSION ELECTRON MICROSCOPY - An Introduction
© Imperial College Press
http://www.worldscibooks.com/materialsci/p703.html

coefficients is not arbitrary and their symmetry is related to the order of the aberration. For instance, there is no second-order aberration of sixfold symmetry. There kind of conditions are the invariant boundary conditions that have to be met, regardless of the notation and definition of the aberration coefficients. Which definition and which notation is chosen should depend upon its usability for a certain application. The important point is that the optics, which is described by the aberration coefficients, is independent of the definition of these coefficients. Table 7.3 compares the aberration coefficients of Haider *et al.* (2008b), Krivanek *et al.* (2009a) and the notation of Pöhner and Rose (1974).

### 7.5.5 *Aberration function and image aberrations*

While the impact of the aberrations on the geometrical wave surface can be described by the aberration function $W$, or alternatively by $\chi$, we are equally interested in the image aberrations $\Delta w_{\mathrm{i}}$ which describe the impact of the aberrations in the image plane for HRTEM imaging or in the specimen plane in the case of STEM imaging. In the previous sections, we introduced the image aberrations $\Delta w_{\mathrm{i}}$ and the aberration function $W$ independently. What remains to be addressed is the connection between image aberration and aberration function, i.e. the connection between the warping of the wave surface and its impact on the image or on the STEM probe. What is the relation between $\Delta w_{\mathrm{i}}$ and $W$?

The electron trajectories are perpendicular to the wave surface. For the case of a spherical wave surface, all trajectories stemming from the spherical wave surface intersect in one single point, which is the Gaussian image point. If the curvature of the wave surface deviates from a spherical surface, the trajectories do not intersect in a single point anymore — an astigmatic image point results. Hence, it must be the gradient of the wave surface which provides information on the position where a particular trajectory passing the aperture in $\omega$ intersects the Gaussian image plane. If the wave surface is spherical, the aberration function $W$ vanishes, i.e. $W = 0$, as well as its gradient. This is the reference state. For a warped aberration function, however, the gradient does not vanish. This means that a given ray does not intersect the Gaussian image plane in the Gaussian image point. This qualitative argument leads us to the quantitative formulation of the relation between the aberration function $W$ and the image aberration $\Delta w_{\mathrm{i}}$ (for a derivation see, e.g. Grivet, 1972; Hawkes and Kasper, 1989a), which can be expressed as

$$\boxed{\Delta w_{\mathrm{i}} = -M\left(\frac{2\partial W}{\partial \overline{\omega}}\right) = -M\left(\frac{\partial W}{\partial \theta_x} + \mathrm{i}\frac{\partial W}{\partial \theta_y}\right),} \tag{7.17}$$

where $\omega = \theta_x + \mathrm{i}\theta_y$ and $M$ denotes the lateral magnification. For the case that the effect of off-axial aberrations can be neglected, $W$ can be replaced by $\chi$.

Equation (7.17) is an important relation which directly relates the shape of the non-ideal geometrical wave surface expressed by $W$ to the effect of the aberrations

ABERRATION-CORRECTED IMAGING IN TRANSMISSION ELECTRON MICROSCOPY - An Introduction
© Imperial College Press
http://www.worldscibooks.com/materialsci/p703.html

in the relevant plane of observation. The image aberration is determined by the derivative of the aberration function in respect to the coordinates in the aperture plane. The image aberration of a particular ray is proportional to the gradient of $W$ or $\chi$. The greater the gradient of $W$ in a position $\omega$ of the aperture plane, the larger is the displacement from the Gaussian image point (see, e.g. Fig. 7.2). This is intuitively understandable by looking, for example, at Fig. 7.11. In Eq. (7.17), we essentially closed the missing connection between image aberrations and the shape of the corresponding wave surface, i.e. its wave aberration.

The derivative in Eq. (7.17) explains that for a given aberration, the sum of the exponents of the ray parameters in the aberration function is one unit larger than the order of the aberration, which is the sum of the exponents of the ray parameters describing the impact of the aberration in the image plane, i.e. its image aberration.

In the following chapter, it will be shown that the multi-pole optical elements employed in aberration correctors have characteristic geometrical (axial) aberrations, like round lenses have. As noticed by Otto Scherzer (1947), these aberrations or, alternatively, these imaging characteristics, can be employed to correct for the intrinsic spherical aberration of the objective lens. On the other hand, the violation of the rotational symmetry of the beam by making use of such multi-pole elements also means that there is a larger number of symmetry-permitted aberrations present. Furthermore, with the correction of the dominant geometrical aberration, i.e. the third-order spherical aberration $C_3$, the sensitivity towards parasitic and residual geometrical aberrations increases. Hence, in an aberration-corrected microscope, up to a certain order, all of the geometrical aberrations in Table 7.2 need to be considered and properly compensated, in order to approach the case of a rotationally symmetric aberration-corrected information transfer.

## 7.6 Summary

In this chapter, we discussed different types of aberrations: chromatic aberrations vs. geometrical aberrations; coherent vs. incoherent aberrations; and axial vs. off-axial aberrations. We also introduced the Seidel aberrations, i.e. the symmetry-permitted geometrical aberrations of a round lens. Based on the geometrical wave surface, we generalized the concept of the aberration function. We showed that aberrations can be described by either wave aberrations or image aberrations, and that these two descriptions can be linked to each other. Keywords for this chapter are: image aberration; wave aberration; aberration function; chromatic aberration; geometrical aberration; axial (or aperture) aberration; off-axial aberration; isoplanatic approximation; Seidel aberrations; order; rank and degree of an aberration; and aberration notations.

ABERRATION-CORRECTED IMAGING IN TRANSMISSION ELECTRON MICROSCOPY - An Introduction
© Imperial College Press
http://www.worldscibooks.com/materialsci/p703.html